24. CRYSTAL MORPHOLOGIES IN BASALTS DREDGED AND DRILLED FROM THE EAST PACIFIC RISE NEAR 9°N AND THE SIQUEIROS FRACTURE ZONE[1]

James H. Natland, Deep Sea Drilling Project, Scripps Institution of Oceanography, La Jolla, California

ABSTRACT

Variations in crystal morphologies in pillow basalts and probable sheet flows sampled from the region of the East Pacific Rise drilled during Leg 54 are related both to differences in composition and to an extreme range of cooling rate experienced upon extrusion. The basalts range in composition from olivine-rich tholeiites to tholeiitic ferrobasalts, and include some more alkaline basalts. The kinetics of crystal growth in some samples appears to have been influenced by the amount of initial superheating (or supercooling) of the magma, or possibly by differential retention of volatiles. Olivine in quartz-normative ferrobasalts apparently formed metastably at high undercooling.

Despite these effects, reliable petrographic criteria are established to distinguish the principal rock types described regardless of the crystallinity and grain size. Microphenocrysts formed prior to pillow formation correspond closely to mineral assemblages inferred from normative plots and variation diagrams to control crystal fractionation at various stages. The details of spherulitic and dendritic growth also provide some clues about composition.

Petrographic evidence for magma mixing is scant. Only some Siqueiros fracture zone basalts contain zoned plagioclase phenocrysts with glass inclusions similar to those used to infer mixing among Mid-Atlantic Ridge basalts. All basalts from the summit and flanks of the East Pacific Rise are aphyric. One possible petrographic consequence of mixing between olivine tholeiites and ferrobasalts—formation of clinopyroxene phenocrysts—is not evident in any fracture zone or Rise crest basalt. Highly evolved ferrobasalts with liquidus low-Ca clinopyroxene have not been sampled, nor does textural evidence indicate that any basalts sampled are hybrid compositions between such magmas and less fractionated compositions. Evidently the sampled ferrobasalts are close to the most evolved compositions that occur in any abundance on this portion of the East Pacific Rise.

INTRODUCTION

This chapter presents a petrographic introduction to basalts drilled during Leg 54 on the East Pacific Rise near 9°N, and in the nearby Siqueiros fracture zone, as well as basalts dredged from the region during two prior Scripps Institution expeditions—Siqueiros and Deepsonde. With the completion of Leg 54, a suite of rocks has been obtained from this small area (Figure 1) which have remarkably diverse compositions, ranging from olivine-rich tholeiites to iron- and titanium-rich tholeiitic ferrobasalts. There are even a few basalts transitional to alkalic-olivine-basalt compositions recovered from the tops of seamounts.

The general petrographic features of these basalts have been summarized in Batiza et al. (1977), Johnson (1979), and the East Pacific Rise Site Report of this volume. In the present paper, however, the exposition will be keyed to photomicrographs in order to illustrate the profound differences in crystallinity, crystal morphologies, and textures that result from the extreme range of supercooling undergone by compositionally diverse submarine lavas as they are extruded onto the deep-sea floor.

This chapter also complements an earlier paper describing basalts from DSDP Site 395 on the Mid-Atlantic Ridge (Natland, 1978). Here, in a concluding section, both East Pacific Rise and Site 395 basalts will be compared to elucidate contrasting magmatic processes on fast- and slow-spreading ridges . The comparison will be based on a combination of petrographic characteristics and compositional data, primarily electron probe analyses of quench glasses. The glass data are presented in

[1] Appendix by Colin H. Donaldson, Department of Geology, University of St. Andrews, St. Andrews, Fife KY169ST, Scotland, and James H. Natland.

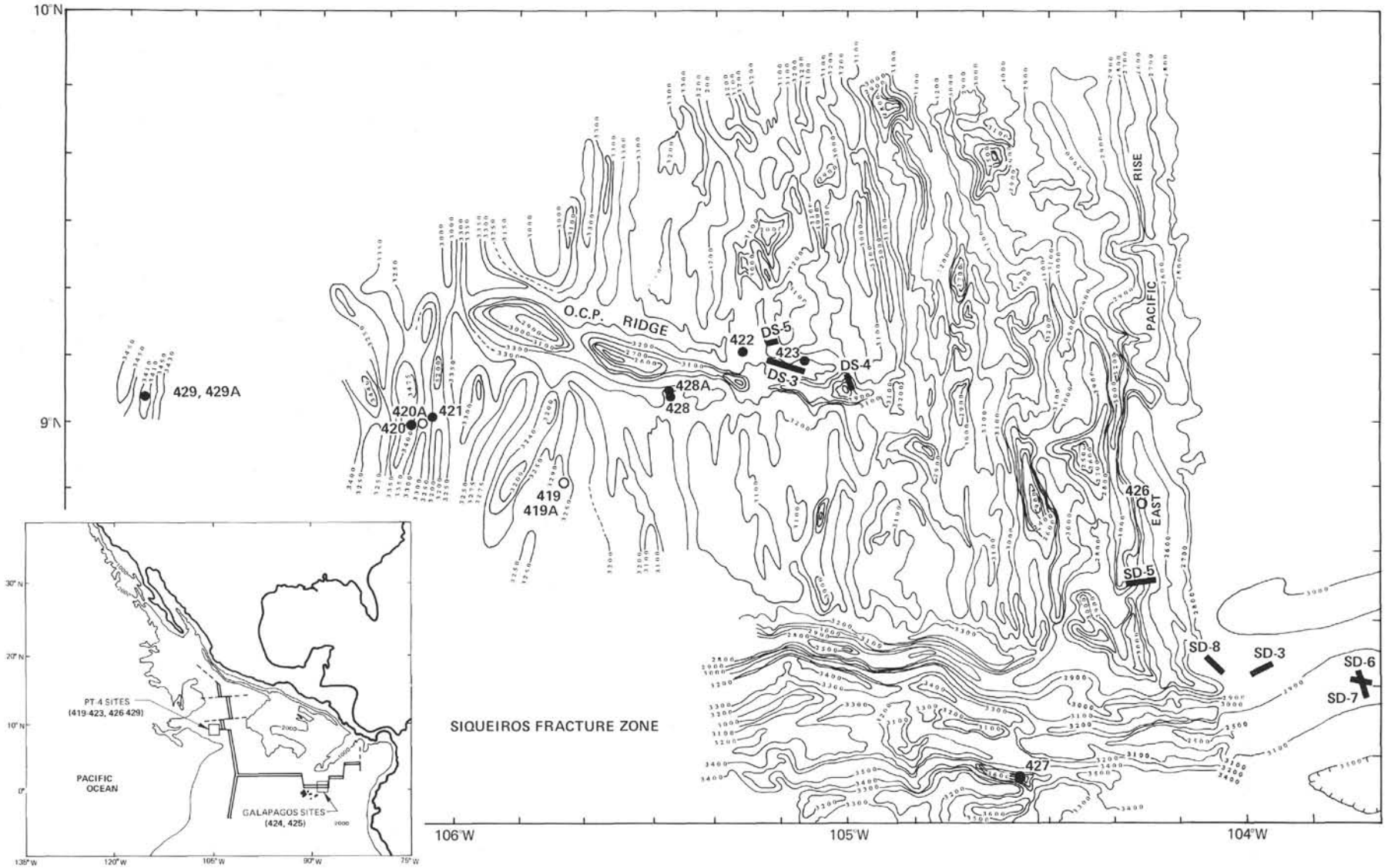

Figure 1. *Bathymetry of the PT-4 site survey area showing the location of dredge stations (SD, DS) and drill sites (Sites 419–423, 426–429). Open circles = no basalts recovered. Contoured by B. R. Rosendahl. Contour interval is 100 meters, except in the Siqueiros fracture zone where some contours have been eliminated for clarity.*

Natland and Melson (this volume) for the East Pacific Rise, and in Melson (1978) for Site 395.

Several studies (Bryan, 1972; Kirkpatrick, 1978; Natland, 1978) have demonstrated the usefulness of providing descriptive information on crystal morphologies to discriminate basalts of different chemical compositions. We are far from understanding all the causes of variation in crystal morphologies, but chemical composition certainly is important and must be considered before other explanations can be assessed. With the recovery of so wide a range of chemical types from the East Pacific Rise, we can approach establishment of reliable petrographic criteria for classification of sea-floor basalts. Such classification, however, cannot be made simply on the presence, absence, or relative abundance of particular minerals. These can be greatly affected by supercooling, or what is more properly termed undercooling.[2] It is therefore necessary to document the various types of crystal morphologies within distinct chemical types through the range of undercooling represented by typical pillows, flows, or intrusive bodies.

Experimental data on olivines (Donaldson, 1976) and plagioclases (Lofgren, 1974) crystallized from basaltic compositions demonstrate that a wide range of crystal morphologies can be systematically related to undercooling. Since undercooling generally is most extreme at a cooling unit boundary (where crystallization is suppressed altogether, so that glass forms), and least in its interior, it makes some sense to describe lavas literally from the outside in, tracing modifications in crystal morphologies and increasing crystallinity as an approximate function of decreasing undercooling. A conceptual basis for this is exemplified by descriptions of pillow basalts by (Kirkpatrick, 1978). He designated several specific zones of crystallization in typical pillows, most of them in the outer few centimeters. These progressed from exterior glass (Zone 1) through isolated spherulites in glass (Zone 2), coalesced spherulites (Zone 3), and thence through two zones of fan and sheaf spherulites, and a final zone of microlitic and skeletal plagioclase, with dendritic clinopyroxene. Natland (1978), although not formally using these zones, traced similar changes in Mid-Atlantic Ridge basalts through to much coarser basalts, with subophitic and ophitic textures.

The same general procedure will be followed here. Six groups of rocks will be described. Most of them are from the Leg 54 drill sites and dredges obtained during the Deepsonde site survey cruise and Leg 54. A few are from Siqueiros expedition dredge hauls. Site and dredge locations are shown on Figure 1 and listed in Table 1. The six groups are:

1) olivine-rich oceanites representing the most primitive tholeiites recovered from either the East Pacific Rise or the Siqueiros fracture zone (dredge SD-7);

[2] Defined as the negative temperature differential, $-\Delta T$, between the equilibrium liquidus temperature and the actual temperature below this at which crystallization occurs; superheating is the positive temperature difference $+\Delta T$ between the liquidus temperature and any higher temperature the melt may have.

TABLE 1
Locations of Leg 54 DSDP Sites and Nearby Dredge Hauls, from Which Basalts Are Described or Discussed in the Text

DSDP Site/Dredge[a]	Latitude (N)	Longitude (W)	Location[b]
420	09°00.10′	106°06.77′	EPR Flank
421	09°01.41′	106°03.68′	EPR Flank
422	09°10.59′	105°16.27′	Base, OCP Ridge
423	09°08.81′	105°06.57′	EPR Flank
424	00°35.33′	86°07.81′	GR Flank
425	01°23.68′	86°04.22′	GR Flank
427	08°06.79′	104°36.35′	SFZ
428	09°02.77′	105°26.14′	Base, OCP Ridge
429	09°02.01′	106°45.87′	EPR Flank
SD-3	08°23.0′	103°57.3′	SFZ
SD-5	08°35.2′	104°17.3′	EPR Crest
SD-6	08°21.5′	103°40.9′	SFZ
SD-7	08°22.8′	103°40.9′	SFZ
SD-8	08°23.8′	104°02.5′	Seamount SFZ
DS-3	09°07.7′	105°07.6′	EPR Flank
DS-4	09°07.0′	105°00.2′	OCP Ridge
DS-5	09°12.6′	105°12.5′	EPR Flank

[a] Latitudes and longitudes are locations where dredges first touched bottom only.
[b] EPR = East Pacific Rise; GR = Galapagos Rift; SFZ = Siqueiros Fracture Zone.

2) olivine-rich tholeiites, also from the Siqueiros fracture zone (dredge SD-7);

3) plagioclase–olivine phyric basalts from the Siqueiros fracture zone (dredge SD-3);

4) aphyric and sparsely phyric olivine tholeiites of the flanks of the East Pacific Rise (DSDP Sites 428 and 429; dredge DS-3);

5) tholeiite ferrobasalts from the flanks of the East Pacific Rise (DSDP Sites 420, 421, 422, and 423; dredges SD-5 and DS-5) and the Siqueiros fracture zone (DSDP Site 427); and

6) "transitional," more alkalic basalts, from OCP Ridge (dredge DS-4).

The first three of these will be considered as a group since they are all porphyritic (in this respect they are comparable to some Mid-Atlantic Ridge basalts), and because they are from closely spaced dredge hauls in the Siqueiros fracture zone. Samples from the crest of the East Pacific Rise, or the typical block-faulted topography on its flanks (the "fabric" of Rosendahl and Dorman, this volume), are substantially aphyric, at least in the sense of lacking macroscopic phenocrysts. The occurrence of porphyritic basalts only in the fracture zone is an important feature of the suite of Rise and fracture-zone tholeiites which will be discussed more fully later.

As in the paper on Site 395 crystal morphologies (Natland, 1978), the terminology used herein is that of Lofgren (1971, 1974) for spherulitic forms in general, and Donaldson (1976) for olivines. Some of the terms of Bryan (1972) are also used.

PORPHYRITIC BASALTS FROM THE SIQUEIROS FRACTURE ZONE

The first two of the rocks to be described were obtained in the same dredge haul (SD-7), and the third was from a nearby dredge haul (SD-3). All were from scarps

some 300–1000 meters deeper than the crest of the nearby East Pacific Rise (Batiza et al., 1977).

The compositions of several dredge SD-7 rocks are listed in Schrader et al. (this volume), who also describe the rocks and give mineral compositions. Natland and Melson (this volume) found that glasses from 10 pillow rims in this dredge haul comprise three distinct compositions (glass Groups D, E, and F of their Table 3). These were among the most magnesian glasses in the entire East Pacific Rise/Siqueiros fracture zone suite. The two rock types to be described here correspond to glass Groups E [Mg/(Mg + Fe) = 0.67] and F [Mg/(Mg + Fe) = 0.71]. Whole-rock compositions listed in Schrader et al. (this volume) are obviously affected by accumulation of olivine crystals, having MgO up to 16 per cent. All the rocks in the dredge haul have abundant, large forsteritic olivine crystals, and even abundant chromian spinel (perhaps 1%). For these reasons, Schrader et al. (this volume) have termed them picrites. However, I follow Macdonald (1949, 1968) in restricting the use of the term picrite to olivine-rich alkalic basalts, and in designating particularly olivine-rich tholeiites "oceanites." This seems especially appropriate for one group of these rocks, represented by glass Group F, which could represent a parental composition for much of the entire rise tholeiite suite (Natland and Melson, this volume).

The third group to be described in this section is particularly rich in plagioclase phenocrysts up to 5 mm in diameter, with lesser olivine phenocrysts. Despite the enrichment in plagioclase phenocrysts, the host glass composition is nearly as magnesian as in the SD-7 basalts. It is represented by glass Group A of Natland and Melson (this volume) with Mg/(Mg + Fe) = 0.66.

Porphyritic Type 1: Oceanite

The whole-rock equivalent of glass Group F is shown in Figure 2. Central to the figure is a full thin-section photomicrograph in transmitted light, in which coarse granular olivine phenocrysts up to 2 mm, olivine glomerocrysts up to 5 mm, and round plagioclase spherulites typically about 1 mm in diameter can be readily seen. Only a few samples of rocks of this type were recovered in the dredge, none coarser grained than this example. The central photomicrograph is oriented with the least crystalline edge toward the top, and is surrounded with an array of more detailed photomicrographs. To the right, photomicrographs show the crystallization features of groundmass olivine of various portions of the sample (Figure 2A, B, and C). To the left are pictures depicting plagioclase spherulites (Figure 2D, E, and F).

The highly magnesian composition of the host glass manifests itself in a remarkable abundance of lattice-type dendrites of groundmass olivine, usually centered on tiny cellular, sometimes swallowtail, olivines (Figure 2A). Within about 0.5 cm further into the rock, the dendritic haloes have completely coalesced (Figure 2B). Still further away from the margin of the sample, where the plagioclase spherulites have coalesced, isolated pockets of interspherulite material have myriads of olivines that form separate, if somewhat feathery, crystals (Figure 2C) of the type termed "lantern and chain" by Bryan (1972).

The plagioclase spherulites, which are brown in color, increase in diameter away from the quench margin of the sample and coalesce at the bottom of the central photomicrograph. Generally, the spherulites consist of three zones: a darker core in which bundles or sworls of plagioclase needles, or even individual plagioclase crystals, can be seen (Figure 2D); a lighter surrounding zone where spherulitic fibers are arranged in radial or cross-cutting patterns; and a darker outer rim where the plagioclase spherulite fibers have intergrown with lattice-type olivine dendrites in miscellaneous orientations. Where the thin section has actually sliced through a central plagioclase crystal, as in Figure 2E, the crystal is surrounded by an additional pale brownish yellow zone where spherulitic fibers are densely packed. The sharp boundary of this inner shell of fibers apparently marks where the nearly parallel fibers diverge sufficiently to have allowed the outer corona of fibers to nucleate upon them. Plagioclase, however, is not the only mineral upon which the spherulitic fibers nucleated. A number of spherulites have olivine and even tiny chrome-spinel cores. These lack the inner annulus of densely packed fibers.

As the diameter of the spherulites increases and they coalesce, individual fibers are coarser and are arranged in more sheaf-like assemblages (Figure 2F). They interfere with each other so completely within the central zone of spherulites that they form distinct subzones with sharp boundaries. Here, too, the outer boundaries of the spherulites are more polygonal and the outer darker zone disappears—a consequence of the formation of discrete crystals of olivine rather than the overlapping olivine dendrites.

The tiny dark spots throughout the thin section (Figure 2G) are optically almost unresolvable. They appear largely to be dark fibers clumping around tiny olivine nuclei, which can occasionally be discerned. The size and density of these spots increase toward the zone of coalesced spherulites where, with the diminished abundance of olivine dendrites, the spherulites overgrow the spots, which become entirely concentrated within the outer third of the spherulites. Since the spots seem to be entirely independent of the fibers of spherulitic plagioclase in these zones, they evidently are not themselves plagioclase. Their abundance suggests them to be clinopyroxene.

Figure 3 depicts various small crystals, mostly olivines, in the rock. Figure 3A is a lantern-type olivine amidst a sea of lattice-like olivine dendrites. Figure 3B is a type of swallowtail olivine, perhaps more appropriately termed "longhorn" olivine. Tiny dendrites can be seen growing from the "horns." Somewhat larger crystals are shown in Figure 3C–E—two of them with spike-like and one with branching dendrites. The crystal in Figure 3F evidently is more tabular than any of these, although faint dendrite arms project from either end. The feature extending the length of the center of the

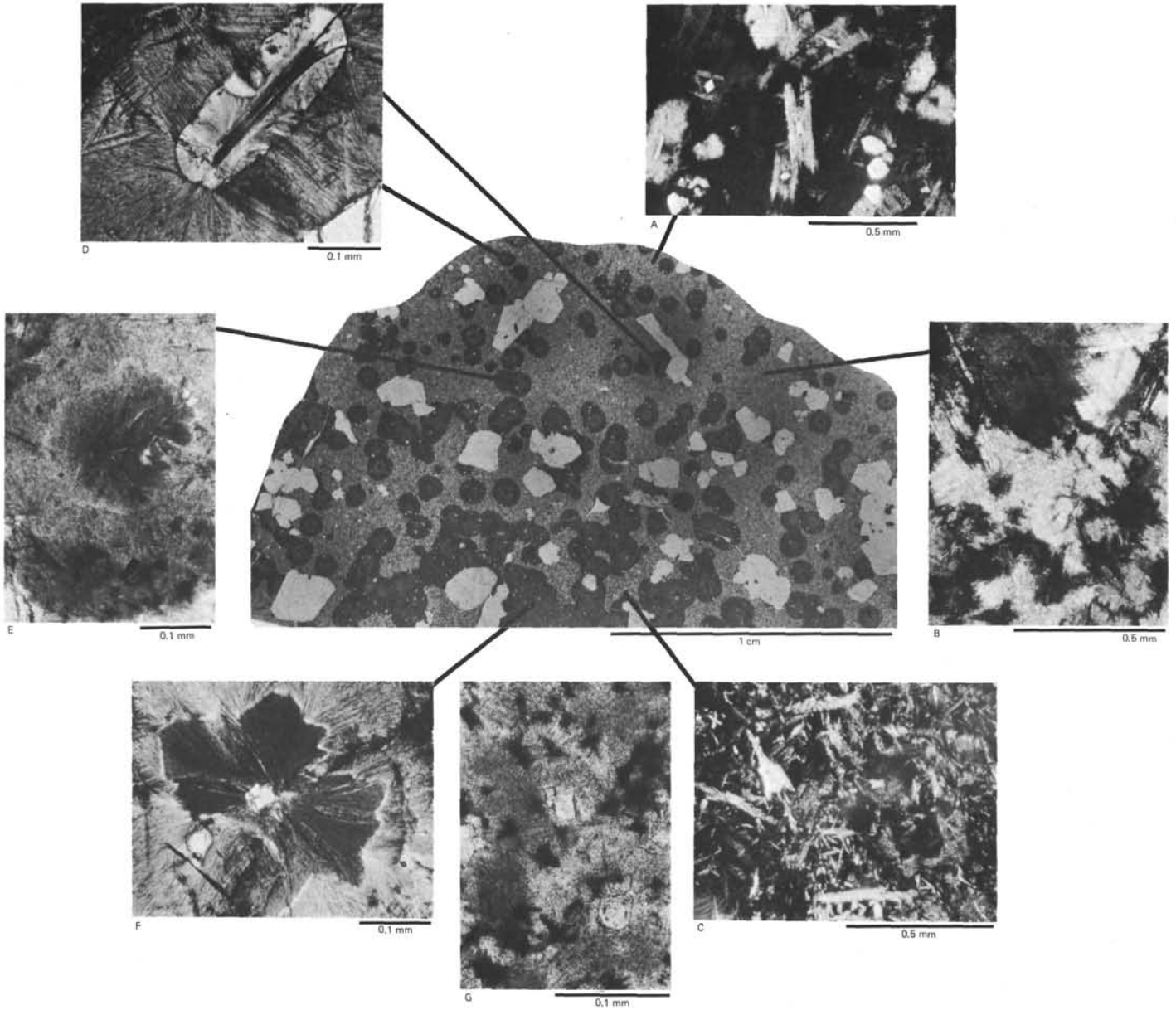

Figure 2. *Photomicrographs of dredge SD-7 oceanite, Siqueiros fracture zone. Central photo is of a full thin section in transmitted light. A–C show details of olivine crystal morphologies, all with crossed nichols. D–F show details of growth of large circular plagioclase spherulites, all in plane-polarized light. G depicts irregular brown dendrites which speckle the lighter colored portions of the sample, in plane light.*

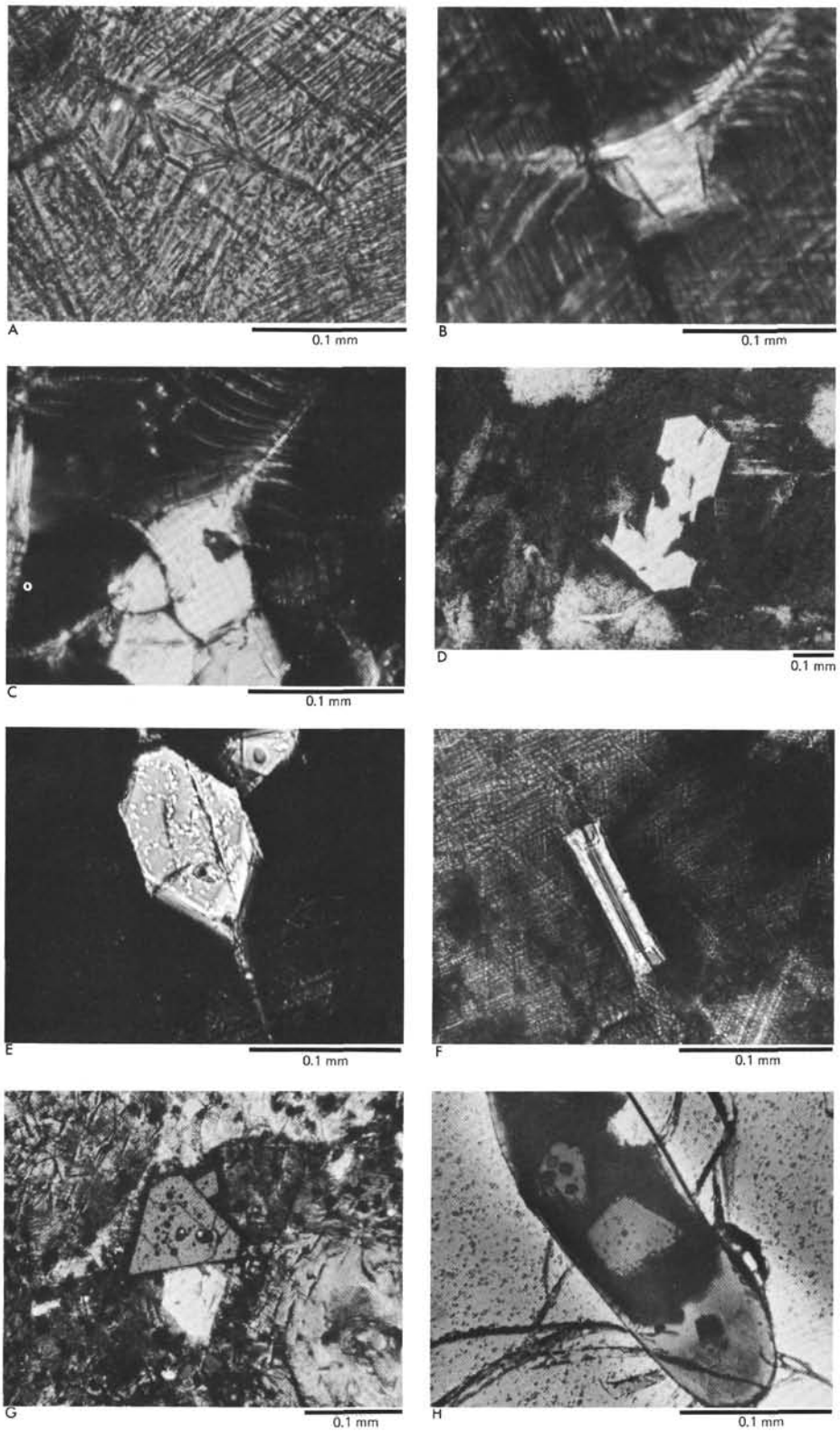

Figure 3. *Small crystals in dredge SD-7 oceanites. (A) Lantern-shaped olivine surrounded by dendrites, plane-polarized light. (B) "Longhorn" olivine with dendrite fibers projecting from horns, crossed nichols. (C) "Christmas-tree" dendritic projections from a small olivine phenocryst in dendritic zone, crossed nichols. (D) Small skeletal olivine microphenocryst in glass with isolated lattice-type olivine dendrites, crossed nichols. (E) Small euhedral olivine crystal with spike-like projections, crossed nichols. (F) Euhedral orthopyroxene (?) in coalesced olivine dendrites, crossed nichols. (G) Euhedral Swiss-cheese chromian spinel, plane-polarized light. (H) Spinel with plagioclase spherulitic overgrowth in glass inclusion within olivine megacryst, plane-polarized light.*

crystal is probably a hollow interior tube. Unless it is in a very unusual orientation, the morphology of this crystal is not like that of olivine. Schrader et al. (this volume) have found tiny orthopyroxene crystals in samples of this rock type using an electron microprobe. The grain in Figure 3F may therefore be an orthopyroxene. Figure 3, G and H, show brown euhedra of chromian spinel, each with spherical inclusions of trapped glass. The spinel in 3H itself is within a glass inclusion in a granular olivine phenocryst. Even so, it is festooned with brown plagioclase spherulitic fibers.

In four thin sections of oceanite available to me, there are no vesicles; and sulfides are very rare. Only the tiniest spherical specks of pyrite and chalcopyrite can be seen, and these are widely scattered.

The patterns of crystal growth can be used to trace the cooling history of the basalt. The granular olivine and euhedral spinel phenocrysts formed under near-equilibrium conditions in some reasonably large magma body prior to extrusion. The extrusive phase had two parts: a period of flow prior to pillow formation, and pillow formation itself. It was during the period of flow that many of the small crystals depicted on Figure 3 grew. The dendritic projections on these crystals, and the dendrite–spherulite groundmass, grew during the final rapid cooling of the outer margins of pillows. In the groundmass, the plagioclase spherulites began growing prior to the olivine dendrites, because the cores of the spherulites are free of intermingled dendritic olivine fibers.

At any given point in the sample, the temperature decreased very steadily and rapidly, but more rapidly toward the margin. Consequently, the interval of undercooling through which relatively well-formed crystals could grow was passed through quickly, but more so toward the margin than in the interior. This explains the increase in both the abundance and size of reasonably well formed crystals toward the interior, the increase in size of the lattice-dendrite coronas around such crystals toward the interior, and the general sequence of dendritic or spherulitic overgrowths on crystals wherever they occur in the section. The chain-like projections of lantern-and-chain olivines are another example of this.

Porphyritic Type 2: Olivine-Rich Tholeiite

The most abundant rock type in dredge SD-7 consists of pie-shaped portions of pillows with distinctly curved glassy margins, and more coarsely crystalline interiors (Figure 4). Olivine phenocrysts are abundant, particularly at the acute apex of each pie-shaped piece, which is also where the average crystallinity is greatest. The pieces conform to the keystone or wedge shape expected from cylindrical or tubular pillows as opposed to sheet flows (see Natland and Rosendahl, this volume, for additional illustrations).

Thin sections made from the top to the bottom of the piece shown on Figure 4 reveal several zones of crystallization conforming to all six zones defined by Kirkpatrick (1978) for Mid-Atlantic Ridge olivine tholeiites drilled at Site 396. Five of these (all but Zone 1, glass) are shown, and labeled Z2 through Z6 on the photomicrographs around the larger picture, which is of a polished rock sample. The characteristics of the zones are given in the Figure caption. Despite the similarity of groundmass zones, the Mid-Atlantic Ridge basalts described by Kirkpatrick were sparsely plagioclase phyric, not rich in olivine phenocrysts.

In the sample shown on Figure 4, microphenocrysts of euhedral olivine and skeletal or tabular plagioclase occur in the glassy rim (Figure 4A, Z2), where they serve as sites for nucleation of partial or complete coronas of brown spherulites (Figure 4B). The myriads of tiny olivine dendrites and the large round spherulites of the oceanite are not present in this sample, which is only slightly less magnesian [Mg/(Mg + Fe) = 0.67 in the glass]. In addition to the euhedral olivine microphenocrysts, olivine with short dendritic projections can be found intergrown with swallowtail plagioclase with spherulitic overgrowths in the glass (Figure 5A). In the zone of coalesced spherulites, many of which are centered on small skeletal plagioclase microlites (Figure 4C), olivine forms tiny scattered euhedral crystals only rarely with thin coronas of dendrites. In zones of fan and sheaf spherulites (Figure 4D), plagioclase is the dominant microlitic mineral, but tiny swallowtail olivines can be seen in addition to the small, more abundant granular olivines. In the coarsest-grained parts of the rock (Figure 4C and F) there are many radial plagioclase arrays centered on granular to euhedral olivines, but some olivine also formed after crystallization of much of the plagioclase. Despite the interference of previously grown crystals, these have an optically continuous branching morphology (Figure 4F). Clinopyroxene in this zone is dendritic (Figure 5B).

The phenocrysts and opaque minerals in these rocks differ also from those previously described in the oceanites. Although many olivines are granular, a good many are skeletal (Figures 5C and 5D); even the granular ones contain large, limpid glass inclusions (Figure 5E). In several pillow fragments that I have examined, all had more olivine, perhaps three times as much, toward pillow interiors than in glassy rims. This evidently was a crystal-accumulation effect.

Spinels are also more abundant toward the pillow interiors, and again they are different from those in the oceanites. They can contain rather large sieve-like glass inclusions (Figure 6A), are darker brown in color, and have skeletal rims (Figure 6B–D). Some even have skeletal interiors (Figure 6E). Titanomagnetite occurs in Zones 5 and 6 as dust-like particles between sheaves or dendrites of pyroxene (Figures 4D, 4E, 6E, and 6F). In the coarsest-grained portions of the samples, they take on skeletal morphologies (Figure 6F) and rim chrome spinels (Figure 6E). Sulfides, chiefly pyrite, are much more abundant than in the oceanites, and occur especially in glassy portions of these rocks where vesicles are decorated with tiny pyrite crystals (Figures 4A and 6G and H).

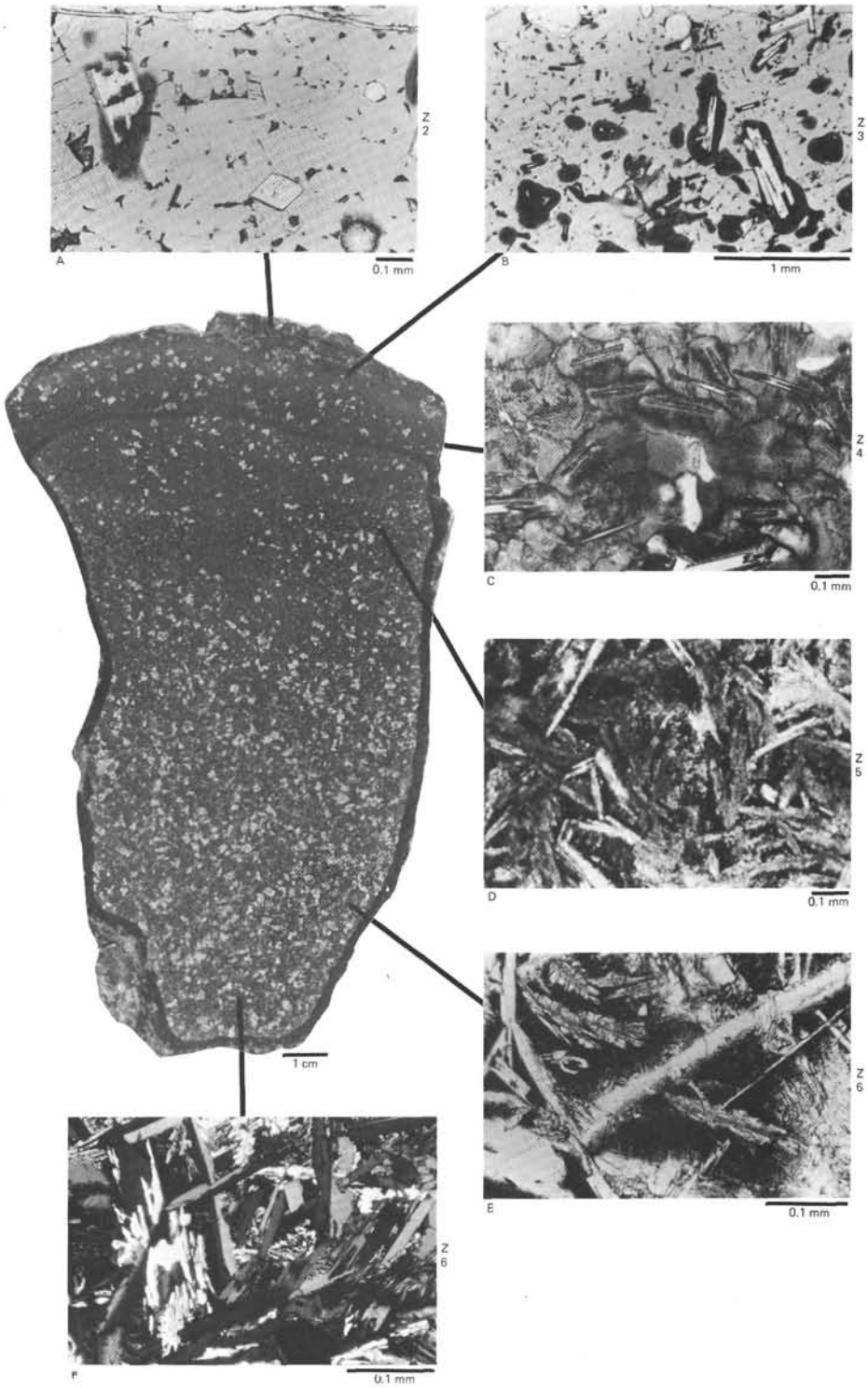

Figure 4. *Crystallization in a porphyritic olivine tholeiite, dredge SD-7, Siqueiros fracture zone. Large photo is of a polished sawed surface of a typical keystone-shaped pillow fragment, glassy edge toward top. A dark oxidation rind surrounds the piece. Photomicrographs are from thin sections made from the same piece. A–E are in plane-polarized light. F with crossed nichols. Lines link photos to general portions of the sample where corresponding textures occur. Zones of Kirkpatrick (1978) are labeled Z2–Z6 as follows: Z2 = glass with crystals and isolated spherulites; Z3 = partially coalesced spherulites with residual glass between; Z4 = fully coalesced plagioclase spherulites with distinct boundaries; Z5 = fully coalesced bow-tie spherulites, here with swallowtail or skeletal plagioclase and swallowtail olivine; Z6 = microlitic plagioclase with dendritic clinopyroxene and branching olivine between.*

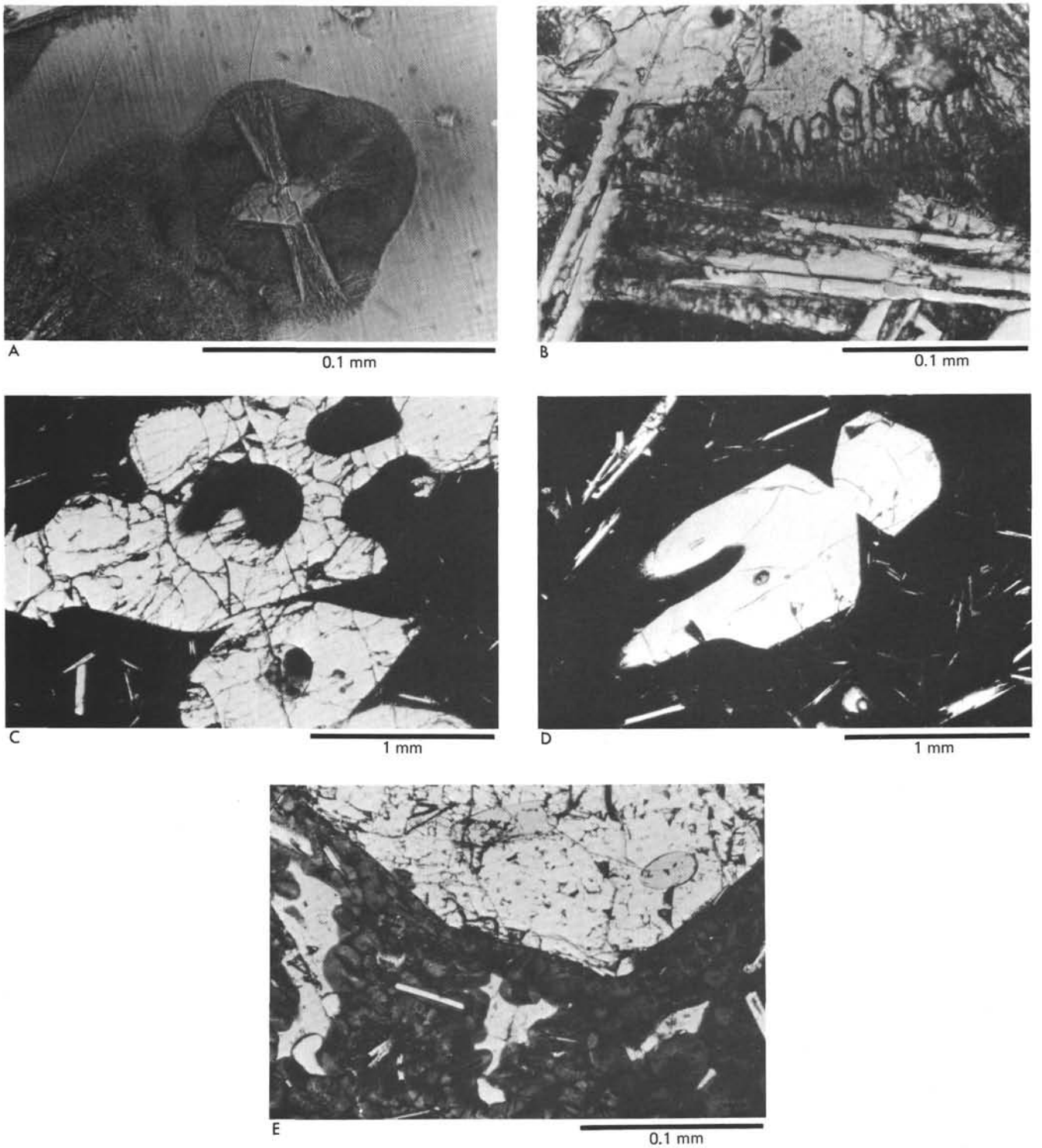

Figure 5. *Features of crystals in dredge SD-7 olivine tholeiites. All photomicrographs in plane-polarized light. (A) Intergrown olivine and swallowtail plagioclase with a corona of intergrown plagioclase spherulite fibers and olivine dendrites. (B) Faceted clinopyroxene dendrites in zone of plagioclase microlites. (C) Portion of a cluster of skeletal olivine phenocrysts in optical continuity. (D) Isolated skeletal olivine. (E) Portion of large euhedral olivine with clear glass inclusions in Z3, zone with coalesced spherulites having isolated glass in between.*

The crystallization history of this sample parallels that of the oceanite. In some fairly large magma body where cooling rates were low, the olivine and spinel phenocrysts formed. Because these crystals have skeletal morphologies, the rate of cooling may have been somewhat higher than for the oceanites, which had mainly granular megacrysts. There were several parts to the extrusion history — periods of transfer to the surface,

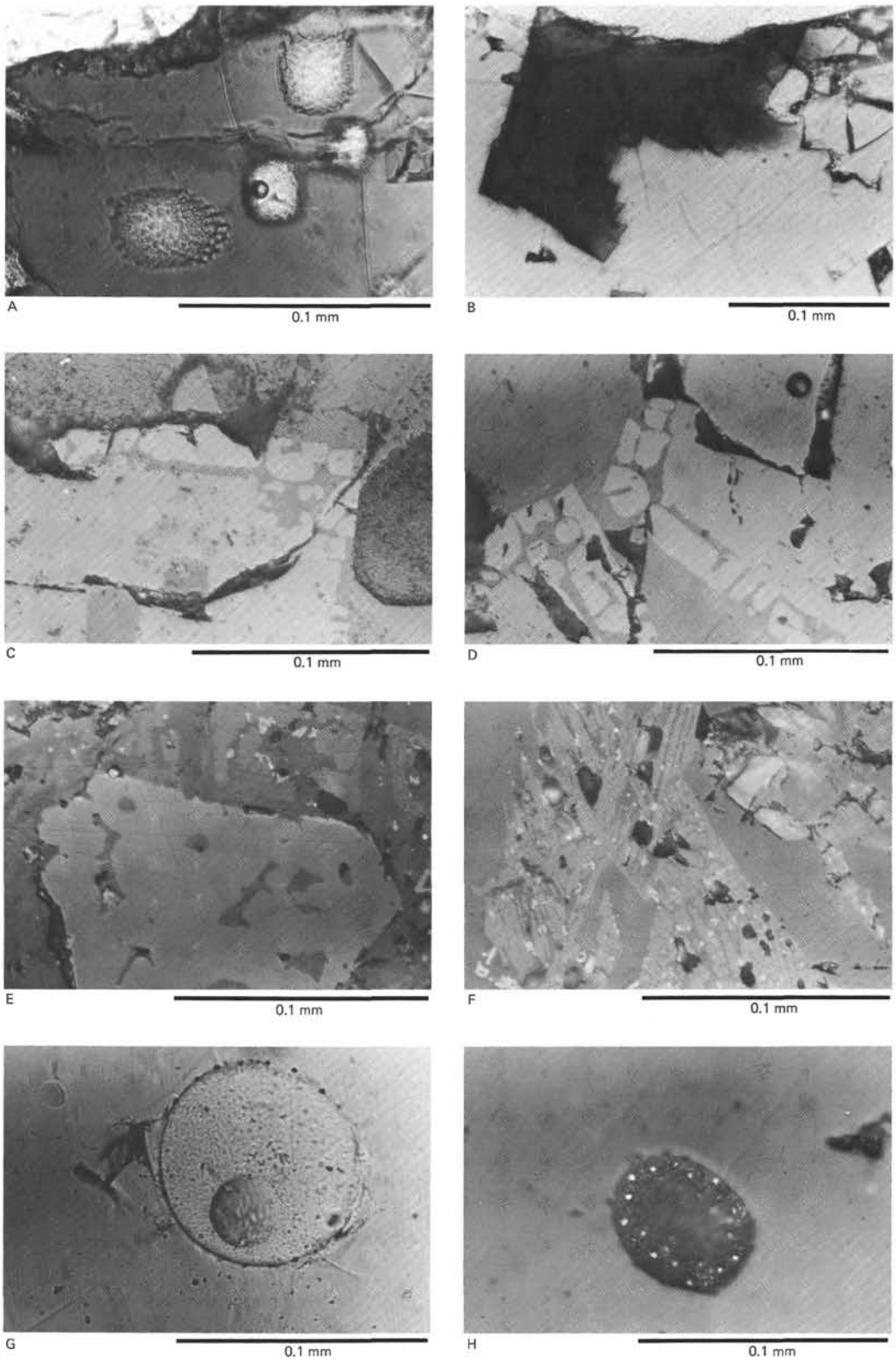

Figure 6. *Oxides and sulfides in dredge SD-7 olivine tholeiites. A, B, and G in plane-polarized light. C, D, E, F, and H in reflected light. (A) Chrome spinel with skeletal border in glass. (C and D) Detail of skeletal chrome spinel borders. (E) Portion of triangular skeletal chrome spinel partly rimmed with titanomagnetite. (F) Small skeletal titanomagnetites in zone of microlitic plagioclase (larger dark gray regions) and dendritic clinopyroxene (light gray). (G and H) Pyrite decorating vesicles in glass.*

eruption, and flow, followed by a final period of pillow extrusion. All were accompanied by successive increases in cooling rate. During transfer, eruption, and flow, olivine microphenocrysts continued to grow, with little change in morphology, although many of the crystals were smaller than the phenocrysts. Spinel continued growing, but in skeletal form. Initial small skeletal plagioclase microphenocrysts started to form. Upon final pillow extrusion, all these crystals were trapped in glass, but both olivine and plagioclase continued to grow to within 1 cm of the edge of the sample. Each portion of the sample passed through an interval of undercooling in which fairly well formed crystals could grow. This was followed by an interval of heightened undercooling in which only spherulitic and dendritic crystals could grow, either as projections of (or overgrowths on) earlier formed crystals, or as separate crystals. Clinopyroxene joined the crystallization sequence, but even so olivine continued to form, in some cases clearly following plagioclase, and sharing interstitial zones with clinopyroxene. In the coarser-grained portions of the sample, crystallization proceeded until interstitial zones departed significantly from the original composition of the melt. Notably, they became more iron-enriched owing to abundant plagioclase formation. Between spherulite bundles, and in interstitial zones, titanomagnetite crystals formed.

Porphyritic Type 3: Plagioclase-Olivine Phyric Basalts

A full thin-section photomicrograph in transmitted light of a plagioclase-rich tholeiite from dredge SD-3 (Table 1, Figure 1) is shown in Figure 7. Individual plagioclase crystals and glomerocrysts up to 0.5 cm across form perhaps 10 per cent of the sample, although overall the rock is more porphyritic than this. The larger plagioclases can be seen to have abundant tiny spherical glass inclusions. Others have fewer, somewhat larger glass inclusions, more irregular in shape. The spherical inclusions are aligned mainly along twin planes (Figure 8A), occurring particularly at the intersection of cleavage planes (Figure 8B). Many of them also contain fluid inclusions.

A number of the somewhat smaller plagioclase phenocrysts are girdled with smaller, granular olivines, which they partly enclose (Figure 8A). The portions of the crystals which enclose the olivines have a marked oscillatory zoning (Figure 8C and D). Fewer zones are present on other crystals. Still others have only a single, narrow, but well-defined, normal zone, which evidently grew at quenching. Chrome spinel is less abundant in this sample than in the two previously described. However, a large plagioclase encloses a spinel grain, itself with a circular cross-sectioned plagioclase intergrowth at its center, on the lower left of Figure 7.

The groundmass of this basalt is very similar to that in olivine-rich tholeiites such as that depicted on Figure 4, and the same type of crystallization zonation can be applied to it. In the plagioclase-phyric rock, however, small lattice-type dendritic olivine overgrowths occur on tiny euhedral olivines in Zone 2 (glass with spherulites) and Zone 3 (coalesced spherulites). Overall, the dendrites are somewhat more abundant than in the olivine-rich tholeiites. The dendrites and spherulites in the outer zones are also similar to those in olivine tholeiite types A_3 and A_4 from DSDP Site 395, Mid-Atlantic Ridge, described and illustrated in Natland (1978), but the dendrites are not as abundant.

SPECULATIONS ON SIQUEIROS FRACTURE ZONE PORPHYRITIC BASALTS

The phenocryst assemblage in the plagioclase–olivine phyric basalts has some resemblance to porphyritic Site 395 basalts, also described in Natland (1978). In those basalts, I identified two generations of phenocrysts, which grew under entirely different conditions. The first consisted of large plagioclase megacrysts and glomerocrysts, containing glass inclusions and having quite calcic cores. The crystals were usually strongly zoned. The second generation of crystals were small, tabular, unzoned plagioclase euhedra and crystal clumps, generally more sodic than first-generation crystals in composition, and without glass inclusions. The two types were postulated to have formed in separate magma batches which were hybridized (Dungan et al., 1978). Natland (1978) proposed that the glass inclusions in the plagioclases, which have primitive, not hybrid or fractionated, compositions (Fujii et al., 1978; Dungan et al., 1978) were trapped during a period of skeletal growth and heightened undercooling in the transfer period from one magma reservoir to another. Kuo (1980) has recently reexamined the Mid-Atlantic Ridge basalts, and concluded that the formation of glass inclusions in the megacrysts occurred as a result of undercooling imparted to a primitive melt as it was mixed with a fractionated melt.

Whatever may be the case, something similar could have occurred here, since there is the same range in phenocryst types, including those with glass inclusions. However, the host glass composition is highly magnesian [Mg/(Mg + Fe) = 0.66; Natland and Melson, this volume], more so than in Site 395 phyric basalts; hence, the extremes in zonation and phenocryst compositions should be less.

Of more importance here is to emphasize that among three magnesian basalt types, with glass compositions differing but slightly, there are two different petrographic types based on the groundmass, yet the two with virtually identical groundmass crystal morphologies have strikingly different phenocryst assemblages. One must suppose that despite small chemical differences, those differences exerted a powerful influence on which minerals crystallized as phenocrysts near equilibrium. As Mg/(Mg + Fe) drops from about 0.71 to 0.66, a transition must occur between crystallization of olivine and spinel alone, to olivine, spinel, and plagioclase together. This impression may be complicated by the possibility that mixing has taken place in the plagioclase-rich basalts. If so, the composition of the melt in which the plagioclase phenocrysts formed may not be the same as that of the present host glass. Further evaluation of this awaits analysis of inclusions in the feldspars.

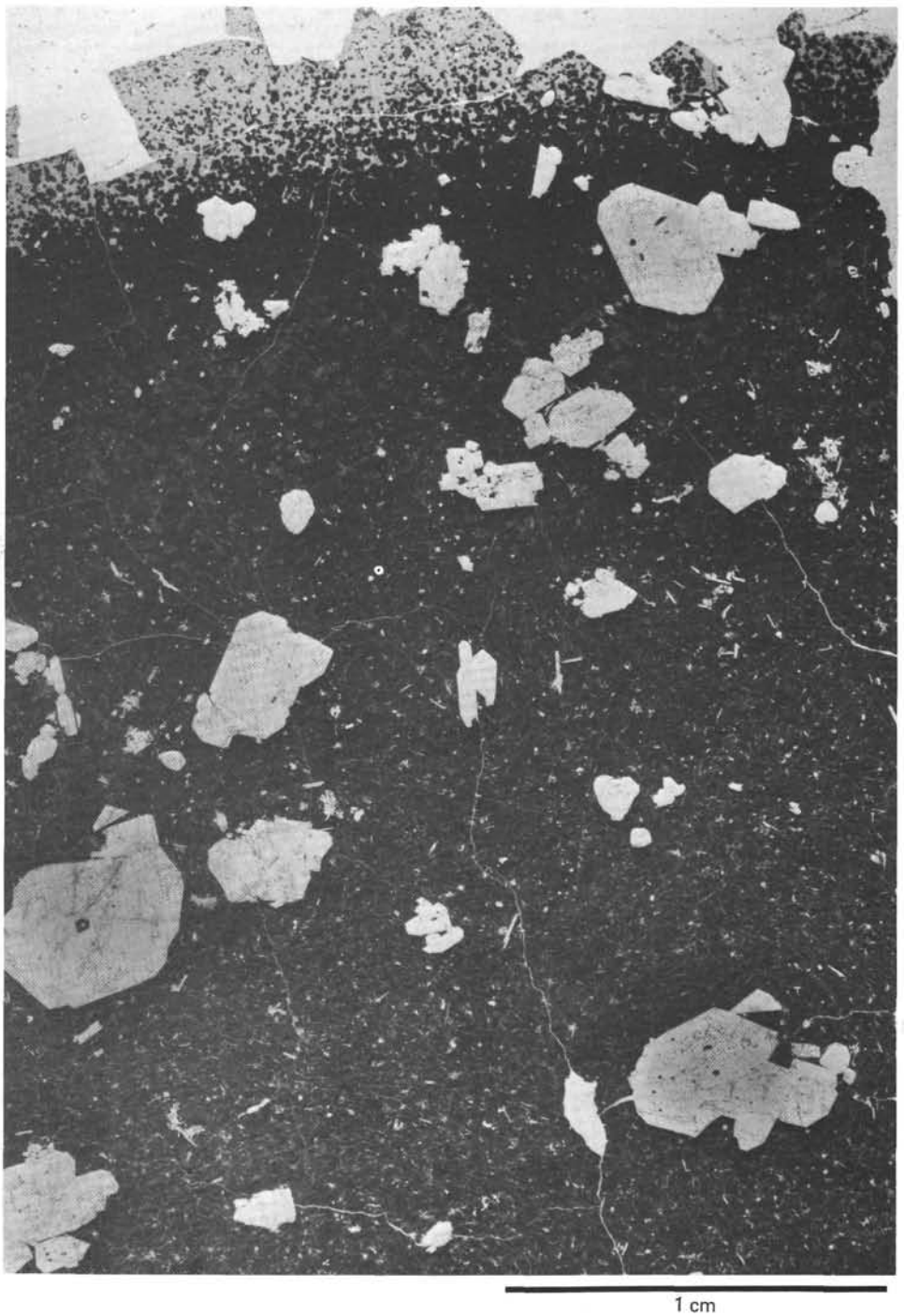

Figure 7. *Whole thin-section photomicrograph of plagioclase–olivine phyric basalt, in transmitted light. Glass with spherulites toward top. Megacrysts are plagioclase with glass inclusions. Medium-sized phenocrysts top center are girdled with small olivines (see Fig. 8). Note increasing size of groundmass plagioclase microlites toward bottom of section. Large megacryst on left margin has a chrome spinel inclusion.*

In whatever way the phenocrysts originated, it is important to emphasize that the glass compositions of the oceanites and the olivine-rich tholeiites cannot be related to each other by fractionation of the phenocrysts in the basalts. They appear to be separate magma batches produced under different conditions of melting or high-pressure fractionation beneath the fracture zone (Natland and Melson, this volume). This may be part of the

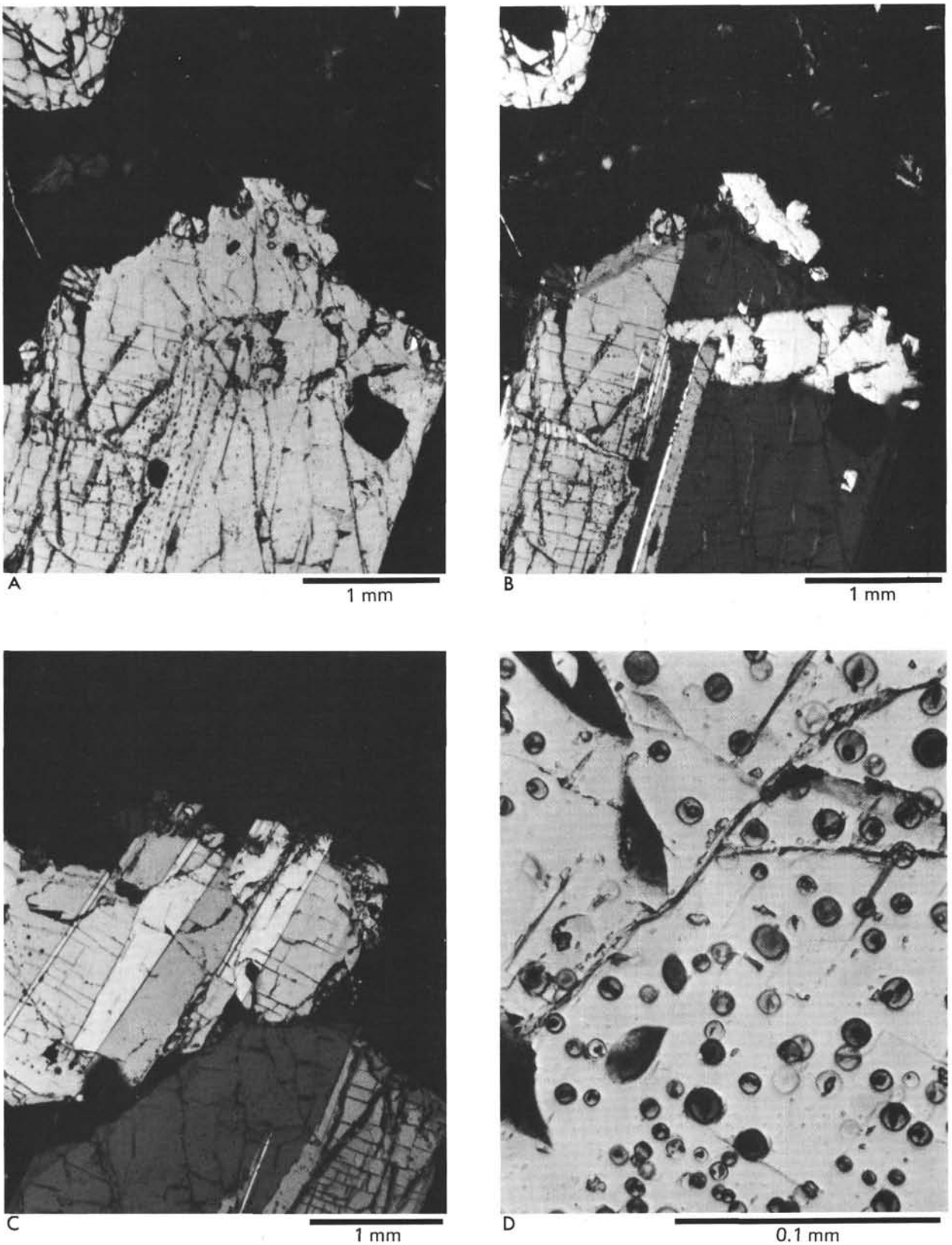

Figure 8. *Details of phenocrysts in plagioclase–olivine phyric basalt shown in Figure 7. (A and B) Zoned plagioclase with glass inclusions with olivines trapped in outermost zone, in plane-polarized and cross-polarized light, respectively. (C) Zoned plagioclase glomerocryst with olivines trapped in rim, crossed nichols. (D) Detail of glass inclusions in plagioclase megacryst.*

reason for the differences in groundmass crystal morphologies, although other explanations are possible (see Discussion).

Schrader et al. (this volume) postulated that the dredge SD-7 basalts leaked laterally into the fracture zone from the base of the axial magma chamber considered by Rosendahl (1976) to underlie this portion of the East Pacific Rise. They implied that a dense, olivine-rich crystal mush could not rise to the apex of such a chamber without losing most or all of its olivines to gravitational segregation into the base of the chamber. This could explain why all sampled Rise and flank basalts are nearly or entirely aphyric. Recently, Sparks et al. (1980) argued that olivine-rich tholeiitic melts injected from the mantle into the base of such a chamber are in themselves both too dense and too viscous (by virtue of being charged with crystals; cf., Shaw, 1972) to convect upward and mix with overlying magmas. The magmas would stay settled at the base of the chamber. This is consistent with the observation of cumulus dunites at the base of ophiolites (e.g., Coleman, 1977; Hopson et al., 1977). The olivines must settle out, and some evolution of the liquid by fractionation must occur before the melt can mix with more fractionated magmas higher in the chamber.

If the Siqueiros fracture zone olivine-rich lavas were tapped from the magma chamber, then, it was probably from its very base. But dredge SD-7 was obtained only 750–900 meters deeper than the summit of the East Pacific Rise axial block, and the deepest parts of the transform fault are only a couple of hundred meters deeper than this (Crane, 1976). Consequently, the mechanics of tapping dense magmas at the base of a magma chamber thought to be some 5 km deep (Rosendahl, 1976) are difficult to envision. Less dense magmas closer to the top of the chamber would seem more accessible. Instead, a separate path from the mantle bypassing the main axial magma chamber is more plausible, especially given the diverse compositions of olivine-rich rocks unrelated by shallow crystal fractionation within the same dredge haul.

It may be of some interest that dredge SD-3, which has basalts so full of plagioclase, was from virtually the same depth interval in the transform fault as dredge SD-7 (Table 1; Figure 1). Fujii et al. (1978) have obtained density and viscosity data on an abyssal olivine tholeiite implying that plagioclase, if formed in similar magmas, should rise in the melt. Moreover, the basalt shown on Figure 7 has sufficient phenocrysts to exceed the threshold abundance (>8%) calculated by Komar (1972) to produce the grain-dispersive effect during dike injection necessary to make flow differentiation a viable mechanism for concentration of phenocrysts. The concentration of olivine phenocrysts toward the base of the olivine-rich tholeiite shown on Figure 4 could even more plausibly be caused by flow differentiation. The phenocryst abundance is sufficient, and many of the pie-shaped pieces exhibit an increased concentration of olivine phenocrysts away from glassy margins. Since some of these pieces must have come from the sides or bottoms of pillows, the distribution of phenocrysts does not seem to be a reasonable consequence of gravitational crystal settling. However, the typical tubular form of pillows, of which the specimen shown on Figure 4 is part of a cross-sectional slice, provides nearly the same constraints on fluid flow as dikes or sills, which are more typical examples of flowage differentiation (Drever and Johnston, 1958; Battacharji and Smith, 1964; Simkin, 1967).

SPARSELY PHYRIC AND APHYRIC BASALTS

The remarkable feature of all the basalts dredged or drilled from the crest or flanks of the East Pacific Rise compared with the rocks described so far from the Siqueiros fracture zone is that they have only very rare macroscopic phenocrysts, or none at all. Thompson and Humphris (this volume) have described euhedral or granular crystals of plagioclase, olivine, or clinopyroxene, singly or in clumps, as phenocrysts, although most are only 1.5 to 2 times larger than what they recognized as groundmass microlites. These phenocrysts invariably occur in the glassy or spherulitic portions of basalts, but not in chemically equivalent holocrystalline samples of the same rocks. The distinction of these crystals as phenocrysts, then, is simply recognition that in most submarine pillow basalts or thin extrusive flows, crystals begin to nucleate prior to final extrusion a few at a time. This is when cooling is nearer equilibrium, cooling rates are lower, and diffusion of components from melt to crystal can proceed at a reasonable pace. Extrusion of pillows or thin flows into cold sea water then traps these crystals at the latest stage of this process. In some samples, though, comparison of the size and abundance of such crystals in glass as opposed to spherulitic or microlitic zones indicates that they continue to grow even within a few centimeters of pillow margins, despite the discontinuity in cooling rate incurred upon extrusion. In a way, the continued growth of these crystals is comparable to normal zoning observed on large megacrysts in porphyritic basalts. Indeed, often the zoning is visible on the smaller crystals (Thompson and Humphris, this volume).

Nevertheless, the small crystals, or microphenocrysts, become surrounded by smaller spherulites or microlites which grow only after the cooling discontinuity occurs. Still, in some samples it is evident that additional crystals of the size and shape of the original microphenocrysts grew from scratch in spherulitic or microlitic zones. Such additional crystals are not present in the glass. This must reflect the propensity of the melt structure to continue its original pattern of crystal nucleation and growth throughout a range of undercooling, despite a marked change in cooling rate. In this case, the customary interpretation of porphyritic texture as indicating a discontinuity in cooling rate breaks down (but only for some of the crystals).

These remarks are offered because they describe in a general way the characteristics of all the Rise crest and flank basalts. In one respect, however, calling these small crystals phenocrysts is misleading. They are not the same as the coarse megacrysts of the basalts described earlier. For this reason, terms such as "micro-

phenocryst" or, if in truly porphyritic basalts, "second-generation phenocryst" are preferable. I shall designate all basalts without macroscopically observable phenocrysts (megacrysts) as aphyric, despite the occurrence and even abundance of microphenocrysts.

Aphyric and Sparsely Phyric Olivine Tholeiites

Samples from dredge DS-3, near DSDP Site 423 (Figure 1) include several phenocryst-poor or deficient olivine tholeiites. Within the dredge, samples DS-3-3 and DS-3-5 have distinctly primitive, high-MgO compositions (Johnson, 1979), and virtually identical petrography. Glass Group H, from DS-3-3 (Natland and Melson, this volume) has the most magnesian composition of any East Pacific Rise tholeiite from this, or any other portion of the Rise analyzed thus far. Natland and Melson (this volume) have proposed that this composition is representative of parental melts supplied from the mantle to the axial magma chamber.

Based on the precision of the electron microprobe analyzing technique, Natland and Melson were unable to distinguish glass Group H from Group F, which represents oceanites from dredge SD-7 in the Siqueiros fracture zone, described earlier (Figures 2 and 3). Given the close similarity in compositions, photomicrographs of sample DS-3-5 (Figure 9) show astonishingly different mineralogies.

Olivine is abundant, to be sure. It occurs as granular and skeletal grains between 0.01 and 0.1 mm in length (Figure 9, A–E). But well-formed plagioclase microlites, absent in the oceanite (Figure 2), occur even in the glass of DS-3-5 (Figure 9A), and olivine dendrites are altogether absent. Brown spherulites follow the pattern of relationship to undercooling (distance from glassy margin) of the olivine-rich tholeiites shown on Figure 4, coalescing first around portions, then around entire grains, of crystals in the glass. This is followed farther away from the quench margin by spherulite growth around cores of plagioclase microlites, then development of sheaf spherulites (Figure 9D and E). The spherulite diameter where they intially coalesce is about 0.1 mm, comparable to that in the olivine-rich tholeiites, but about a factor of 10 less than in the oceanites (Figure 2).

These basalts are also an example of the continued growth of crystals which started to grow before extrusion as pillows. They have extremely elongate acicular plagioclase crystals in glass (Figure 9A and B), but only rare tabular, more equant crystals. Such tabular crystals, however, are abundant in the spherulitic and microlitic zones away from glass rims (Figure 9D and E), and must represent continued growth of the crystals present prior to pillow formation. Moreover, the slender microlites seen in the glass when traced into the pillow interior can be seen first to acquire spherulitic and then dendritic projections at each end, then to become sites for attachment of parallel crystals with similar dimensions in microlitic zones. Olivine microphenocrysts, on the other hand, are neither noticeably more abundant nor larger away from the glassy margin. They also have the same granular or skeletal "hopper crystal" morphologies as in glass (compare Figure 9C and E).

One important feature of this primitive olivine tholeiite is its tendency to have granular or skeletal olivines and skeletal or microlitic plagioclase clustered together, even in glass (Figure 9B). The clumps are too small, too far apart, and crystallized too close to the final stages of extrusion of the basalt for crystal accumulation processes to have been responsible for the clumping. The clusters evidently reflect the tendency of the melt structure to become ordered in some places over large distances (several crystal lengths) before nucleation and during crystal growth. They are an important feature of all basalts which have two phases — plagioclase and olivine, or plagioclase and clinopyroxene — crystallizing together. This type of multiphase heterogeneous nucleation is a probable consequence of cotectic crystallization; I shall argue later that this can be an important indication of the degree of evolution of a basalt.

Aphyric Olivine-Poor Tholeiites Transitional to Ferrobasalt Compositions

Basalts from DSDP Sites 422, 428, and 429 chemically are intermediate between the basalts so far described, and the preponderance of basalts recovered by drilling from the East Pacific Rise, which are sufficiently enriched in Fe and Ti to be termed ferrobasalts (Natland, this volume). Inspection of Table 15 (modal analyses) compiled in the East Pacific Rise Site Report of this volume shows that most of the basalts from Sites 422 and 428 are highly crystalline. They are coarse grained, with ophitic textures. Olivine, though present, is rare, and apparently was subject to *in situ* crystal settling in these rather massive flows or intrusives, to judge from the variability in the modes (0–9.4%). Site 429 basalts, however, were apparently pillows or thin flows, and have substantially the same petrographic features as the more primitive olivine tholeiites described to this point, but with less olivine.

One feature of the petrography that may reflect the greater iron and titanium enrichment of these olivine basalts is that titanomagnetite is an important and obvious mineral, concentrated especially between fibers of fan or sheaf spherulites (Figure 10A), and at the intersections of such spherulites (Figure 10B and C). They are not nearly so abundant in the corresponding zones of the more magnesian olivine tholeiites, but are similar to titanomagnetites in aphyric olivine-basalt types A_2 and A_3 from DSDP Site 395, Mid-Atlantic Ridge (Natland, 1978) which had comparable, moderately evolved compositions.

Tholeiitic Ferrobasalts

Basalts with 1.8–2.5 per cent TiO_2 and >10.5–12 per cent FeO* were cored at Sites 420, 421, 422 (below the massive olivine tholeiites), 423, and 427 (Figure 1). They were also recovered in dredges SD-5, SD-6, DS-3, and DS-5. Those at Sites 420, 421, and 423 have surprisingly similar glass compositions (Natland and Melson, this volume). The greatest enrichment in iron and titanium occurs in basalts from dredge SD-6 and DSDP Site 427

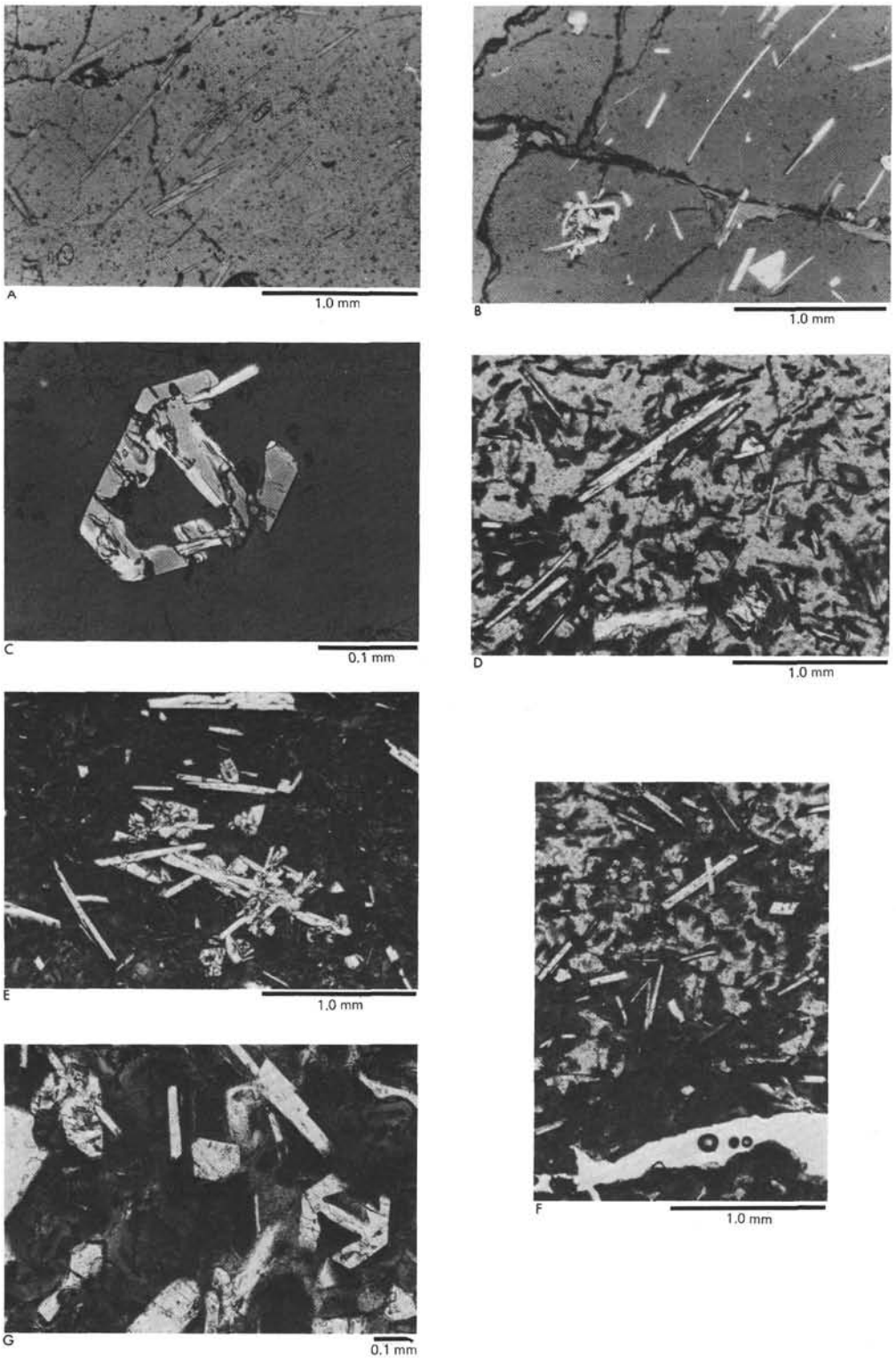

Figure 9. *Crystals in aphyric olivine tholeiites dredge DS-3. (A) Acicular plagioclase needles and granular to euhedral olivines in glass, plane-polarized light. (B) Curved acicular plagioclase and small olivine–plagioclase clump in glass, partially crossed nichols. Curvature of plagioclases occurred during stretching of pillow rim as it grew. (C) Skeletal olivine partially enclosing plagioclase microlites in glass, crossed nichols. (D) Spherulitic overgrowths on microlites, plane-polarized light. (E) Clump of plagioclase and olivine crystals in spherulitic zone, plane-polarized light. (F) Tabular plagioclase crystals with dendritic arms merging with groundmass sheaf spherulites, in plane-polarized light. (G) Assorted tabular plagioclase and euhedral to skeletal olivines in zone of coalesced spherulites with distinct borders, in plane-polarized light.*

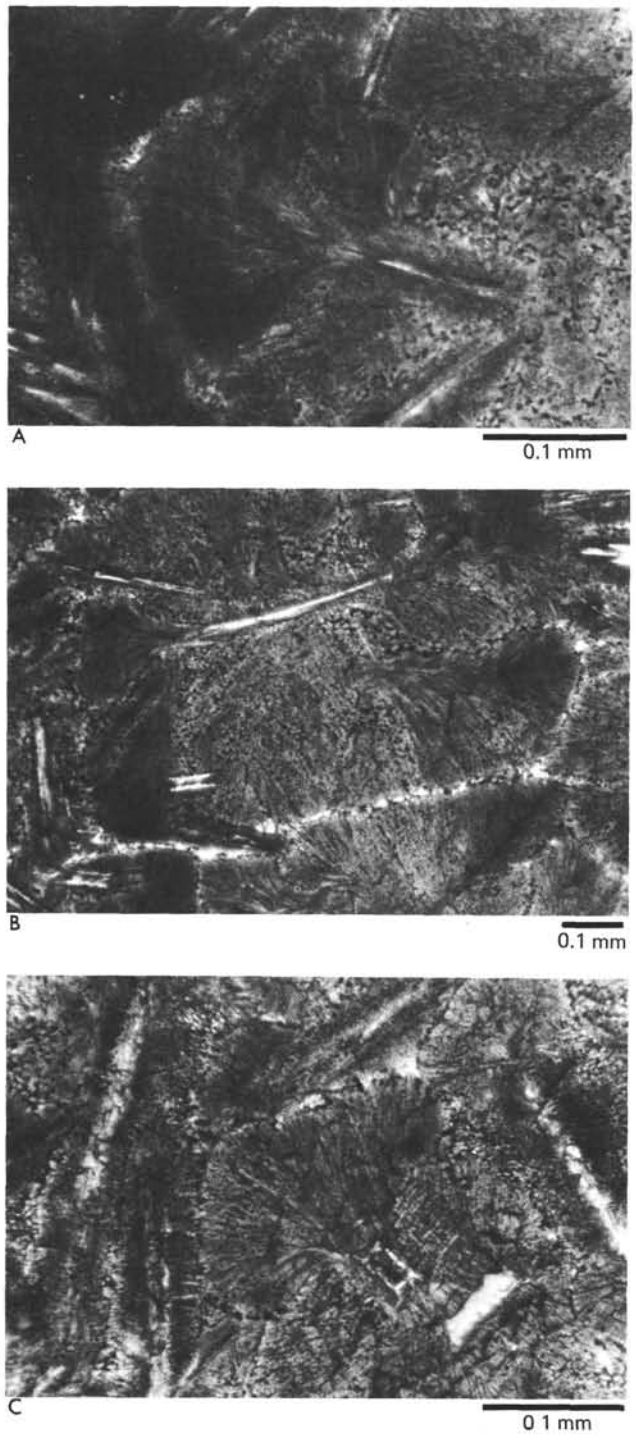

Figure 10. *Examples of fan and sheaf spherulites with titanomagnetites between them in moderately fractionated olivine-poor tholeiite, Hole 428A, all in plane-polarized light.*

(see Natland, Axial Magma Chambers chapter, this volume). In addition to these East Pacific Rise samples, compositionally similar basalts (but with lesser TiO_2 and more FeO*) were recovered at DSDP Site 424 on the Galapagos Rift (corresponding to glass Group T of Natland and Melson, this volume).

Except for the massive ponded ferrobasalts cored deep in the Siqueiros fracture zone at Site 427, all the ferrobasalts recovered by dredge and drill were fragments of pillows, or more probably, sheet flows (see Natland and Rosendahl, this volume, for discussion and illustrations). The characteristics of such fragments are first of all that they have a flat, or nearly flat, glassy margin; secondly, that they have primary consolidation joints orthogonal to the glassy edge, with paralleling alteration rinds; and thirdly, that the pieces are small, with primary joints separated by distances averaging less than the diameter of the core. One such piece is shown in Figure 11. The photomicrographs arrayed around the photo of the rock sample are from several different sites and samples, but each is representative of the general portion of the rock sample indicated on the figure.

The photomicrographs show that the same general zonation scheme used by Kirkpatrick (1978) and applied earlier to olivine tholeiites also can be applied to ferrobasalts, with the following modifications:

1) Glass has a distinctly yellower cast than in olivine tholeiites, and has a hackly pattern of microfractures; crystals within it are clumps of small euhedral and skeletal plagioclase, and anhedral clinopyroxene (Figure 11A).

2) The zone of isolated spherulites (Figure 11B) is narrow, and the spherulites are very dark brown. There is no zone where crystals float free in glass without a dark corona of spherulites.

3) The spherulites coalesce to a zone that is virtually opaque (Figure 11B and C).

4) In the zones of more coarsely fibered spherulites, and in microlitic zones, titanomagnetite forms large grains in high concentrations within reddish brown glass between sheaves of brownish clinopyroxene (Figures 11D and E).

5) Where textures are sufficiently coarse to be termed subophitic, titanomagnetites are very large (up to 0.25 mm) and very abundant, with granular, skeletal, or "staircase" exterior morphologies (Figure 11F and 12A). In comparable zones of olivine tholeiites, they are much smaller (no more than 0.05 mm) with skeletal morphologies.

6) Also in subophitic ferrobasalts, sulfied globules are both more abundant and larger than in olivine tholeiites (Figures 12B and 12C; see also Schrader et al., this volume).

The spherulites in and near glass owe their dark color primarily to abundant, very tiny titanomagnetites. These can be seen only at high magnification using unfiltered, high-intensity, focused convergent light (Figure 12D and E) or reflected light (Figure 12F). These tiny crystals are so abundant that they undoubtedly explain the high intensity of magnetization of the basalts. In detail, spherulites around crystals consist of two zones — a darker interior zone where abundant titanomagnetites occur between plagioclase spherulite fibers, and an outer less dark zone where spherulite fibers are extremely fine, and titanomagnetites are less abundant and in some samples cannot be resolved. Evidently,

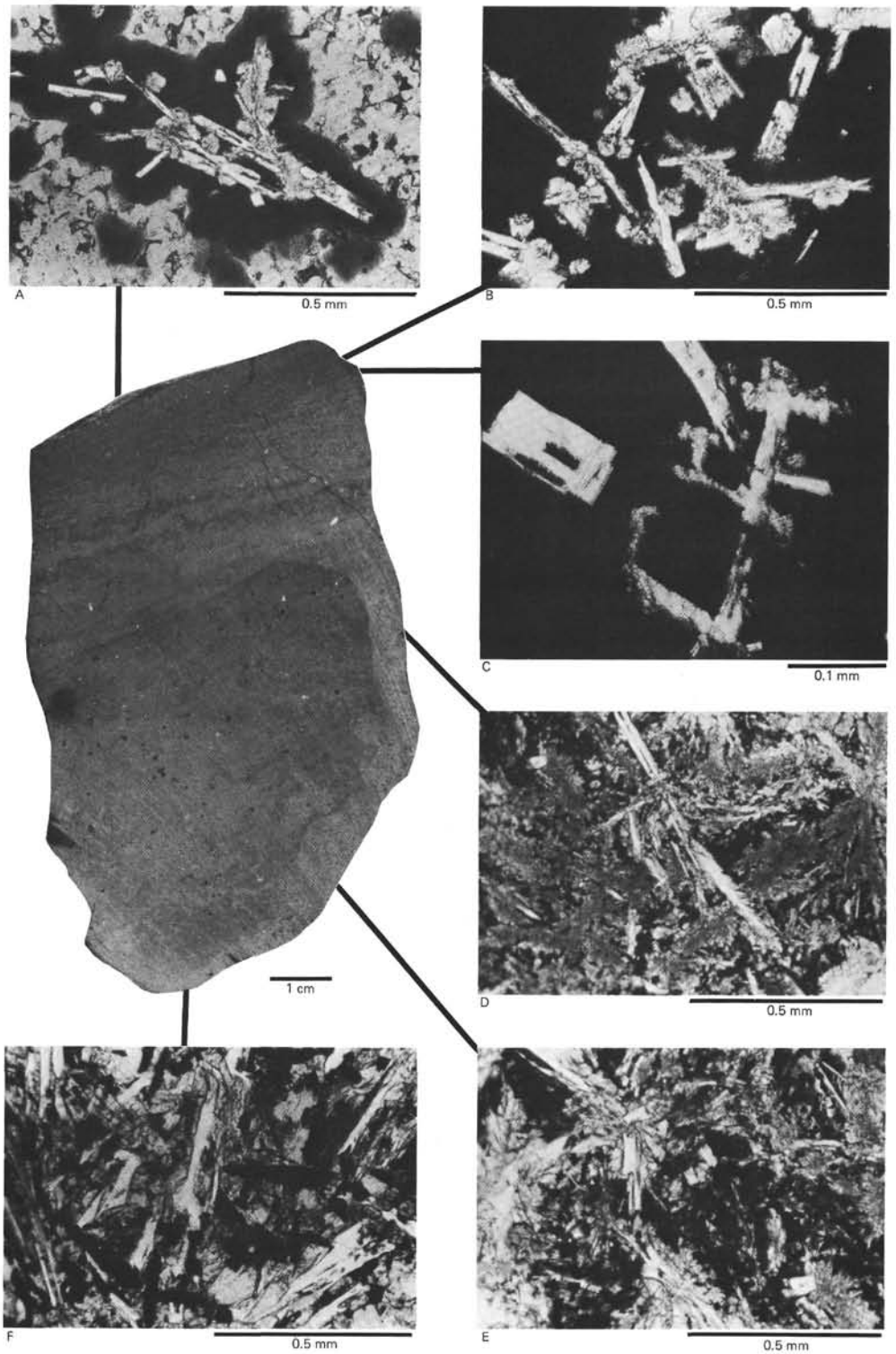

Figure 11. *Crystal growth in ferrobasalts. The rock shows the typical nearly flat glassy top (partially beveled by rotation against another rock during drilling) and faint alteration rind of fragments of small sheet flows or pillows. The photomicrographs are from different samples and show variations at increasing crystallinity and grain size away from the glassy margin, all in plane-polarized light. (A) Plagioclase–clinopyroxene crystal cluster in glass with dark brown corona of spherulites. (B) A similar crystal cluster in the zone of nearly opaque coalesced spherulites. (C) Skeletal olivine and smaller skeletal plagioclase in zone of coalesced spherulites. (D–F) Transition from crudely fan-like clinopyroxene spherulites and plagioclase microlites to nearly ophitic mesh textures in the same thin section. Note high concentration and coarse grain size of titanomagnetites between sheaves of clinopyroxene in D and E, and between larger crystals in F. Sample data: A = Sample 423-8-1, 4–8 cm, Piece 1; B = Sample 421-2-1, 12–17 cm, Piece 2; C = Sample 420-15-1, 15–19 cm, Piece 3; D–F = Sample 421-7-1, 145–148 cm, Piece 21.*

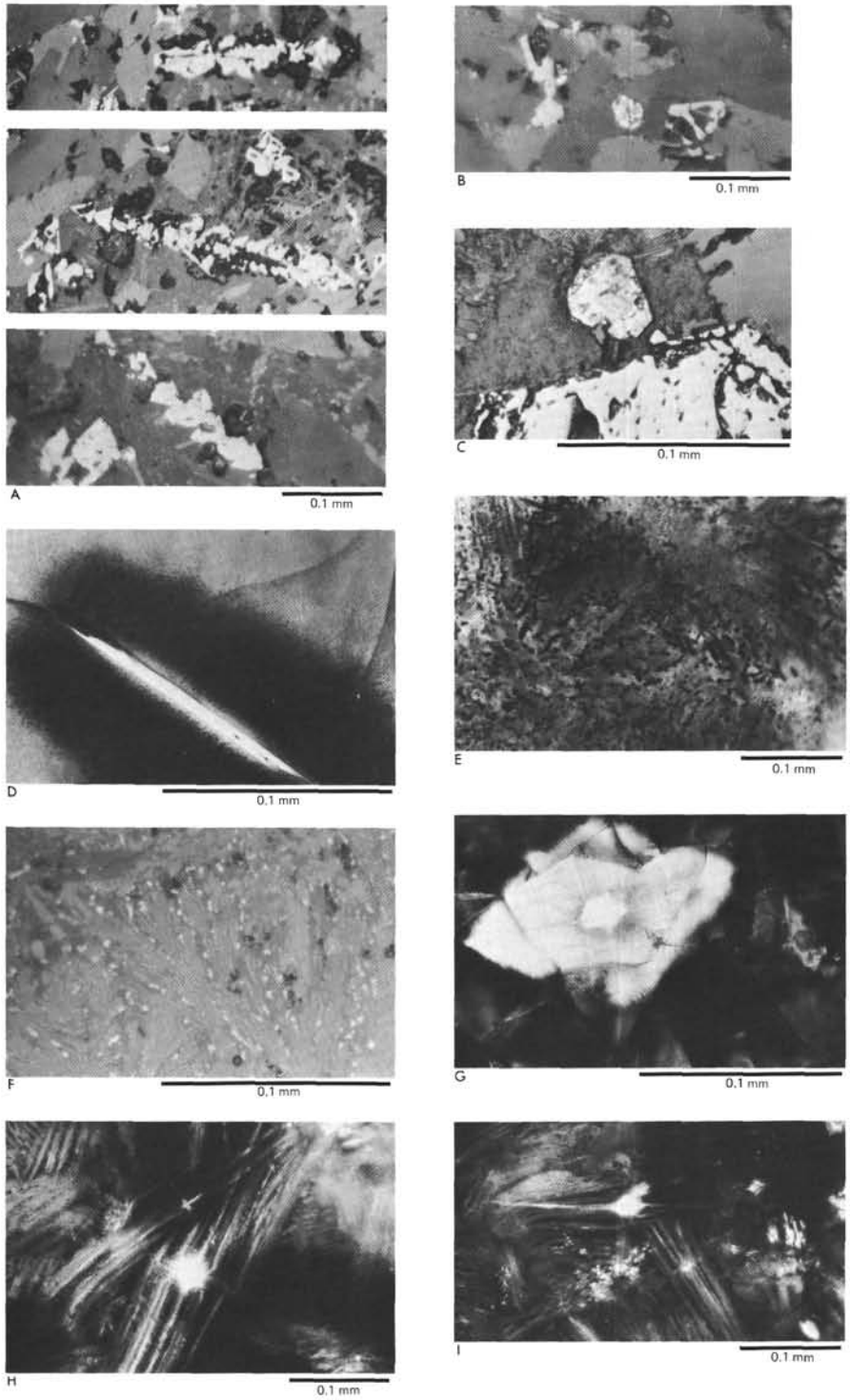

Figure 12. *Details of growth of spherulites and opaque minerals in ferrobasalts. (A) Collage of photomicrographs showing skeletal "staircase"-type titanomagnetites from the same sample, reflected light. (B and C) Examples of sulfide spherules in subophitic ferrobasalts, reflected light. (D) Isolated spherulite in glass with tiny titanomagnetites. (E) High magnification detail of zone of coalesced spherulites showing abundance of titanomagnetites between silicate fibers, plane-polarized light. (F) Tiny titanomagnetites in zone of coalesced spherulites, reflected light. (G) Spherulite with dendritic interior structure, plane-polarized light. (H) Dendritic fibers grown from diamond-shaped clinopyroxene, plane-polarized light. (I) Lantern-and-chain olivine in zone of coalesced spherulites and dendrites, plane-polarized light. Sample data: A. Sample 420-14-1, 0–8 cm, Piece 1; B. Sample 420-14-1, 0–8 cm, Piece 1; C. Sample 427-9-5, 78–80 cm, Piece 6b; D. Pleiades dredge 2D, Sample 3, East Pacific Rise crest 3° 25'S; E. Sample 421-2-1, 12–17 cm, Piece 2; F. Sample 427-9-1, 0–7 cm, Piece 1; G. Sample 421-2-1, 12–17 cm, Piece 2; H. Pleiades dredge 2D, Sample 3; I. Sample 421-2-1, 12–17 cm, Piece 2.*

growth of the silicate fibers so enriches glass between them in iron that titanomagnetite must form.

The spherulites are probably composites of both plagioclase fibers and clinopyroxene dendrites. In certain cross sections, they have an interior dendrite framework. (Figure 12G). In coalesced zones the dendrite fibers are coarser, and grew from tiny diamond-shaped clinopyroxenes (Figure 12H).

Olivine can occur in these basalts, but it is very rare and only occurs in near-glassy samples within the dark, nearly opaque mesostasis. In all cases that I have examined, it has either skeletal or lantern-and-chain morphologies (Figures 11C and 12I). Modal data (Table 15, East Pacific Rise Site Report) show that it does not occur in more crystalline samples. Here is possibly a case analogous to crystallization in the pure diopside system where olivine precipitates metastably, ahead of clinopyroxene, at high undercoolings (Kirkpatrick and Melchior, 1979). Since glass compositions in these basalts are quartz-normative, and thus supposedly incompatible with the growth of olivine, metastable olivine crystalization seems likely.

The occurrence of olivines in these basalts complicates any classification scheme based solely on the occurrence of minerals, particularly olivine. The various criteria listed earlier all seem more reliable as petrographic indicators of ferrobasalt composition.

Transitional-Alkalic Olivine Basalts

The "transitional" (term of Johnson, 1979) basalts recovered in dredge DS-4 from near the summit of one peak on OCP Ridge combine some of the attributes of ferrobasalts with some of those of olivine tholeiites. Olivine is present, even as tiny crystals in glass (Figure 13A), but does not form coarse megacrysts or glomerocrysts. The largest crystals are small euhedra grouped in small clumps (Figure 13B). These olivines enclose abundant, but tiny, euhedral chromian spinels (Figure 13C). There are no free-floating spinels apart from the olivines, as there are in the olivine tholeiites. In glass, the small olivines lack dendritic coronas.

Despite the olivine, the initial spherulites formed in glass are brown and very dark. They coalesce to a dark brown mesostasis, reminiscent of ferrobasalts. They are small, elongate, and distinctly fibrous in glass (Figure 13D) where they are arrayed in rows or sworls (Figure 13E). These apparently are a consequence of stretching of the cooling yet still plastic skin of the newly forming pillows. In detail, the spherulites in the glass can be seen to consist of two types: small ellipsoidal bundles of tiny radial fibers, and still smaller, equally dark fibrous bundles with wisp-like dendrites branching laterally from them (Figure 13D). The two types may be variations on a theme, representing cross sections of different-sized spherulites, or cuts in different directions. They do not coalesce around acicular or needle-like plagioclases further into the rock, nor around any other optically identifiable mineral. They are probably clinopyroxene. This impression is reinforced by the development within 1–2 cm of glassy margins of striking, distinctly different sheaves and bundles of spherulitic plagioclase (Figure 13F and G). These have a dark corona with abundant titanomagnetites where their outer, finely fibrous extremities intersect the coalesced equivalents of those so prominent in the glass. The two types of spherulites combine and interdigitate farther into the samples, where they are joined by tiny lantern and chain olivines with lattice-type dendrite coronas. Ultimately, these give way in microlitic zones to acicular plagioclase, extremely elongate swallowtail and hopper olivines, and very fine dendritic clinopyroxene (Figure 14A and B). Here, the olivines form nuclei to radiating plagioclase clusters (Figure 14C) and can assume extremely elongate morphologies (Figure 14D and E).

To recapitulate, the distinctions between these basalts and ferrobasalts are: (1) these have abundant olivine and associated chrome spinel, and (2) they lack plagioclase–clinopyroxene crystal clumps in glassy and spherulitic zones. The distinctions between these basalts and olivine tholeiites are: (1) lack of plagioclase microlites, or crystal clumps of olivine and plagioclase, anywhere in the samples; (2) lack of isolated plagioclase microphenocrysts or megacrysts; and (3) presence of a dark zone of coalesced spherulites, probably including clinopyroxene spherulites, a type absent or rare in typical olivine tholeiites.

DISCUSSION

The foregoing descriptions raise a number of important questions. It is evident, for example, that very similar, if not identical, melt compositions can be host to mineral assemblages with different crystal morphologies and different mineral proportions at comparable distances from cooling unit boundaries. Why?

Given this fact, there are two corollary questions. At what level do compositional differences dictate crystal morphologies and mineral assemblages in a way that cannot be altered beyond recognition by kinetic effects? Are there any reliable petrographic criteria that can be used to distinguish ferrobasalt from olivine tholeiite in all cases, or the latter from more alkalic olivine basalts?

Finally, we can ask in what way petrographic data on these basalts constrain magmatic processes on the East Pacific Rise, particularly crystal fractionation, mixing, contrasts between the Rise and the fracture zone, and differences between the Rise and the Mid-Atlantic Ridge?

These questions are considered in turn in the following paragraphs.

Similar Compositions — Dissimilar Crystal Morphologies

The question of the influence of melt composition on the formation of phenocrysts has already been discussed. The porphyritic basalts are all close to the transition between crystallization of olivine alone, and cotectic crystallization of olivine and plagioclase. This transition occurs over a very narrow compositional interval.

There are really only two types of groundmass textures among the olivine-bearing and olivine-rich basalts: that in the oceanites on the one hand, and all the other olivine tholeiite types on the other. Although the oceanite is clearly more magnesian than several of these,

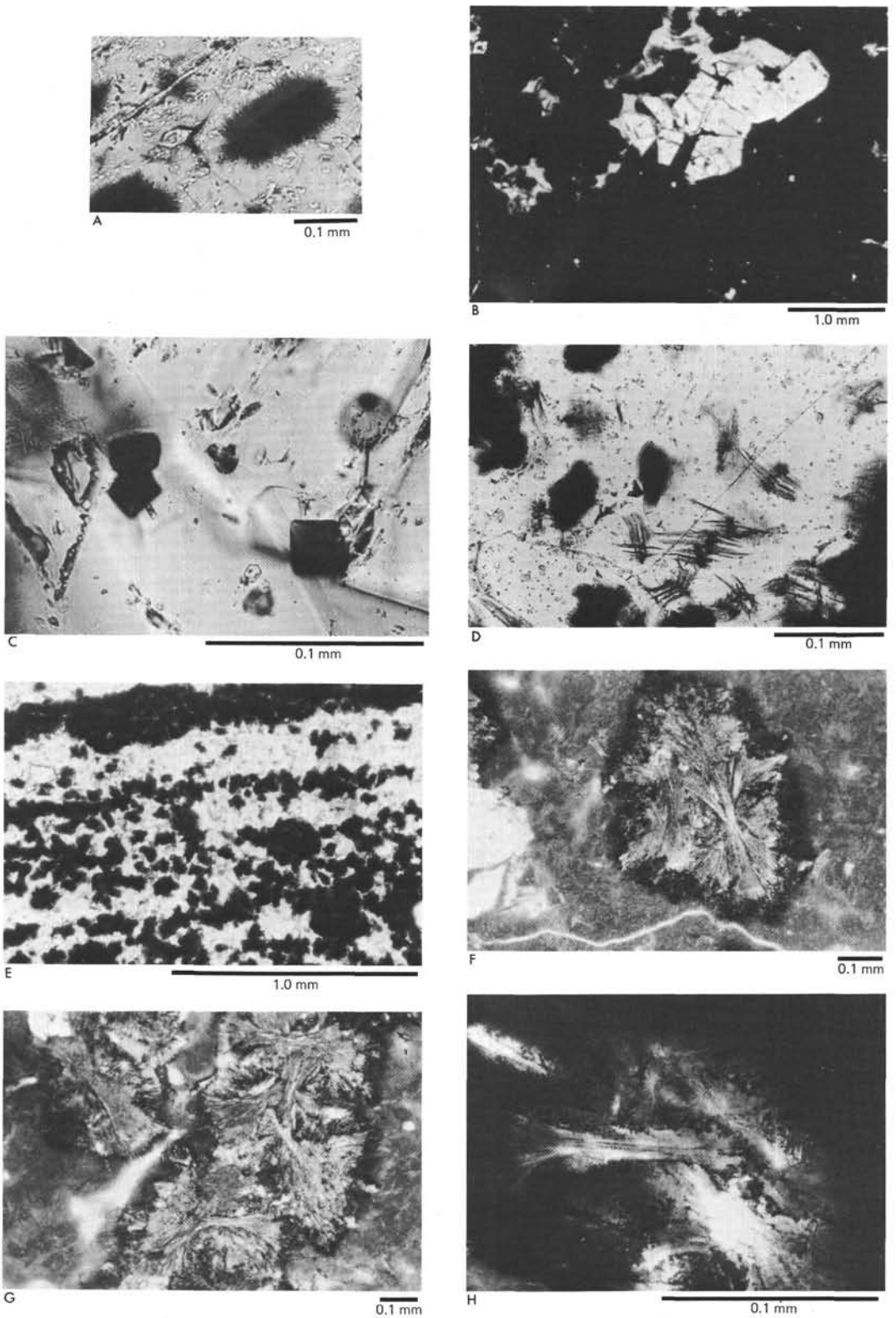

Figure 13. *Crystal growth in "transitional" basalt, dredge DS-4, OCP Ridge. All photomicrographs are in plane-polarized light unless otherwise designated. (A) Individual fibrous spherulite and small lantern-type olivine crystal in glass. (B) Clump of euhedral and granular olivine phenocrysts in zone of coalesced spherulites. (C) Chrome spinels enclosed in olivine microphenocrysts. (D) Dark brown dendrites and larger rounded dark brown spherulites in glass. (E) Aligned spherulites in glass. (F) Plagioclase sheaf spherulite with dark border rich in titanomagnetite. (G) Cluster of several sheaf spherulites. (H) Detail of titanomagnetite enrichment in outer border of sheaf spherulite.*

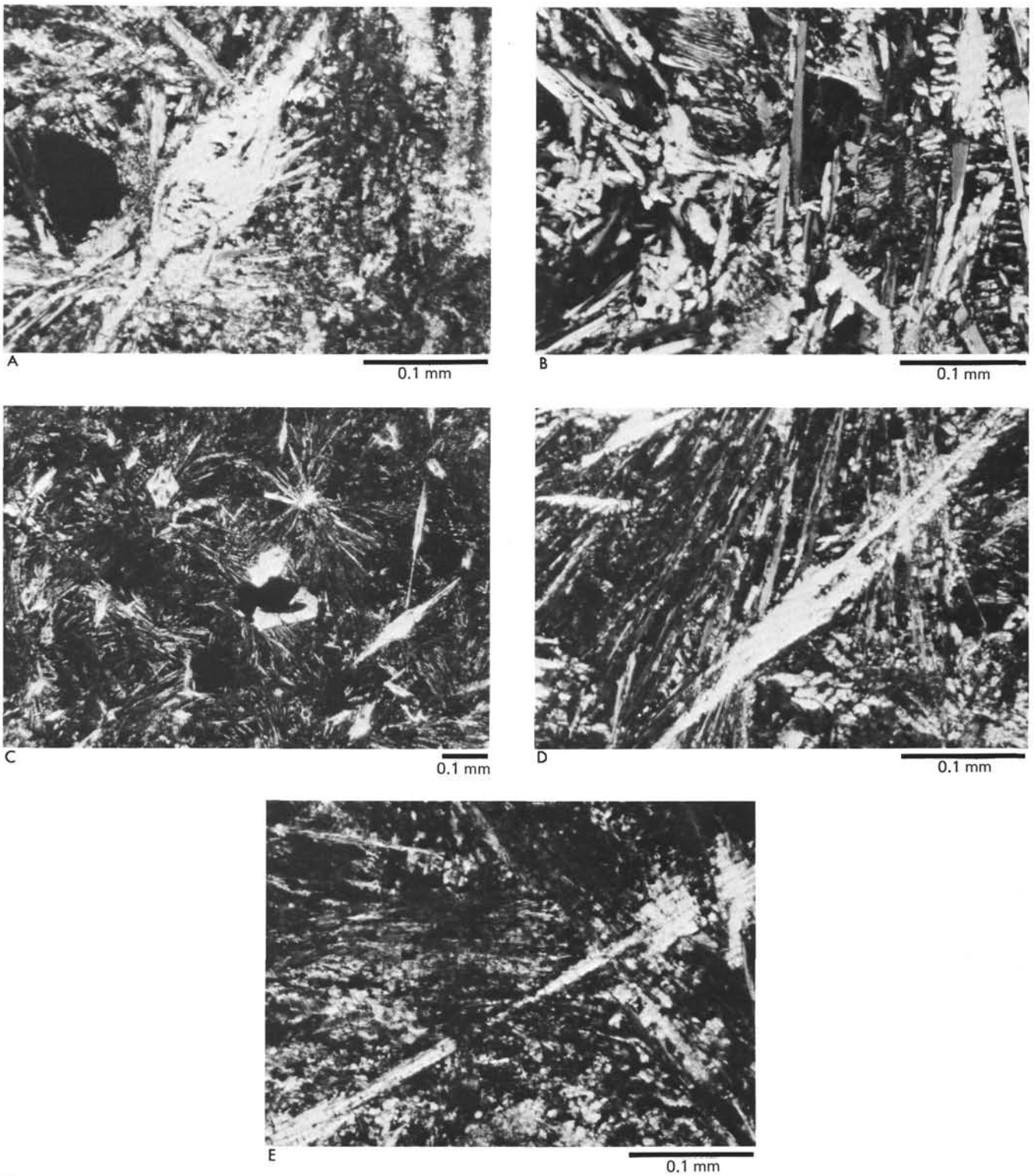

Figure 14. *Crystal growth in microlitic zones of "transitional" dredge DS-4 basalts. (A) Hopper-type olivine crystal in microlitic groundmass, crossed nichols. (B) Representative microlitic groundmass texture, showing acicular plagioclases and fine, dendritic clinopyroxene between plagioclases, crossed nichols. (C) Radial plagioclase microlites centered on an olivine nucleus, crossed nichols. (D and E) Examples of extremely elongate olivine crystals, crossed nichols.*

there is virtually no difference in its glass composition and the composition of aphyric olivine tholeiite glasses from dredge DS-3 (Natland and Melson, this volume), as already discussed. There are at least four possibilities why plagioclase microlites are so abundant in the glass of the DS-3 basalts, but are not present in the oceanite.

1) *The compositional differences, though small, were critical.*

The magnitude of the compositional difference is virtually undetectable in the glasses, and it is in any case much smaller than the wider range of compositions found among all other olivine tholeiites. These have groundmass textures similar to DS-3 basalts, but not the oceanites. Donaldson (1979), however, has cautioned that major changes in melt structure result from small compositional changes, and these in turn can produce major differences in crystallization, particularly in the delay in nucleation of olivine.

2) *The lack of vesicles in the oceanite (possibly related to deep extrusion in the fracture zone) implies that volatiles have not exsolved from the melt and this prevented plagioclase from forming.*

Volatile retention, especially of water, may be important, especially considering that there may have been as much as 1000 meters difference in depths of eruption of the two basalts, preventing vesicle formation in the oceanites. Thompson and Humphris (this volume) proposed just this mechanism to explain anomalously calcic plagioclase cores in plagioclase microphenocrysts of drilled ferrobasalts. They are not convinced that water is a much less abundant component of dissolved volatiles in East Pacific Rise magmas than carbon dioxide (Moore et al., 1977; Delaney et al., 1978; Muenow et al., 1979). Also they pointed to the fact that gas-bubble inclusions have only been analyzed from melt trapped by skeletal crystal growth of olivine and plagioclase megacrysts, perhaps grown in the mantle or deep crust. They view the large axial magma chamber thought to underlie the crest of the Rise (cf., Rosendahl, 1976) as a likely place where water could be added to the melt, especially given the importance of hydrothermal circulation of sea water in cooling the magma chamber (Corliss et al., 1979). They argue that p_{H_2O} would drop during the rise of magmas from the top of Layer 3 to the ocean floor. The magmas vesiculated en route to the surface, causing strong normal zoning on the plagioclase microphenocrysts. Magma ascent and eruption were too rapid to allow the unstable calcic plagioclase cores to resorb; instead they were zoned.

This argument has some appeal here, especially if the oceanites were tapped from within the magma chamber, and did not vesiculate en route to the surface. But because the magmas were so much less fractionated than those examined by Thompson and Humphris (this volume), the effect of p_{H_2O} on shifting the plagioclase liquidus boundary actually tended to suppress its crystallization at high undercooling.

Unfortunately, there are no data on gas-bubble inclusions for these samples. The lack of water in any analyzed inclusions in abyssal tholeiites, and the general low vesicularity of the Rise tholeiite suite cast some doubt on this whole line of reasoning. Also, as previously discussed, density–depth relationships make it difficult to envision tapping basalts so rich in olivine phenocrysts from the axial magma chamber; instead, as argued earlier, a route bypassing the magma chamber seems more likely. Thus although volatile retention is a possible explanation for the contrasting petrography of the two basalt types, it clearly needs further investigation.

3) *The delay in the nucleation of plagioclase with respect to olivine in the oceanite was caused by eruption of a somewhat superheated magma; the aphyric olivine basalt, however, was not superheated.*

Donaldson (1979) showed that the delay of nucleation in olivine even at considerable undercooling is a function of (1) cooling rate, (2) melt composition, and (3) amount of initial superheating. He pointed to somewhat similar experimental data of Gibb (1974) that showed that plagioclase nucleation at a given undercooling is even more sluggish than olivine, and can cause olivine to crystallize first in a basalt with plagioclase on the liquidus. Extreme undercooling is known to increase the temperature interval between olivine and plagioclase crystallization in a lunar picrite (Walker et al., 1976). For the dredge SD-7 oceanites and dredge DS-3 primitive aphyric olivine basalts, we can presume that pillow cooling rate and melt composition are virtually identical (with the possible exception of water contents, as discussed above), leaving superheating as the remaining alternative explanation.

Donaldson (1979) described the growth of olivine in melts as dependent on the development of random "olivine-like" embryos, 0.01 to 0.05 mm across. He described embryos as " 'clusters' of ions, some of which have the structures of solid phases which can crystallize from the melt." With increasing superheating, embryo size decreases, causing longer "incubation periods" before olivine nucleates at any given undercooling. Walker et al. (1979) also found that superheating decreases the number of nucleation sites (i.e., embryos). Donaldson (1979) additionally found that crystal morphologies in basalts of the same composition will vary at the same rate of undercooling, depending on the initial superheating.

These conclusions imply that the oceanite could have erupted with some superheating, whereas the aphyric olivine basalt my have been slightly supercooled. If plagioclase nucleation is more sluggish than that of olivine, then the oceanites may be viewed as basalts which would have formed well-crystallized microlites in glass were it not for initial melt superheating. Neither plagioclase microlites nor spherulites formed readily because the embryos of plagioclase nucleation were reduced in number and size. This also no doubt dictated the larger size of plagioclase spherulites at comparable distances from the glassy rim in the oceanite compared with the olivine tholeiite. Centers of nucleation were few and far between, and appear to have been small crystals (olivine, spinel, plagioclase microlites) far larger than the crystals which served as centers for nucleation of olivine dendrites. Either the size or the type of interface was critical in determining where the spherulites grew. In the

dredge DS-3 aphyric olivine basalts, nucleation embryos and crystals were far more abundant; hence, the spherulites were much smaller. This particular melt composition may never have undergone much superheating, and the growth of olivine prior to eruption and pillow formation could have diminished the number of olivine embryos to the extent that few dendrites formed.

4) *The oceanite has abundant olivine phenocrysts, the primitive olivine basalts do not.*

Donaldson (1979) observed that addition of olivine crystals (phenocrysts) to a melt reduces the number of crystallization embryos by depolymerization of melts. This would explain the large and rare plagioclase spherulites in the oceanite, but seems contradicted by the myriads of olivine crystallites and dendrites. Also, most of the basalts in dredge SD-7 (shown on Figures 4–6) have olivine phenocrysts, but lack the groundmass texture of the oceanites.

In summary, the possibilities for producing different crystal morphologies and proportions of minerals at high undercooling are considerable, and are far from being dependent solely on composition. Of the alternatives just discussed, that of contrasting magma superheating and supercooling has the fewest objections for the samples in question, but none of the alternatives has been entirely precluded, and they could be important factors in controlling crystal growth in these and other samples.

Petrography as a Guide to Composition

Despite the important kinetic effects just described, there are still aspects of the petrography of sea-floor basalts that can be related to composition. Natland and Melson (this volume) discerned two types of chemical variation within the suite of glasses from basalts dredged and drilled from the region. These were (1) crystal fractionation, first of plagioclase and olivine, then with clinopyroxene adding to the assemblage, and finally with plagioclase and clinopyroxene together, and (2) variations among olivine basalts caused by differences in the depth or degree of melting, and source heterogeneities. These two types of variation are indicated by arrows on a ternary plot of normative olivine, diopside, hypersthene, and quartz (Figure 15). The figure emphasizes variation of the two principal mafic phases, clinopyroxene and olivine, in modifying residual glass compositions during fractionation. The fractionation trend is indicated schematically by the sharply curved arrow (labeled 1). The double-headed arrow (labeled 2) shows the approximate range among tholeiites caused by variations at the source. Natland and Melson (this volume) also presented MgO variation diagrams which show the same general features, including on many diagrams changes in curvature analogous to the fractionation trend of Figure 15.

In this normative projection, the initial importance of olivine as an early-fractionating mineral, and of clinopyroxene as a late-fractionating mineral, are clearly evident. Glass Groups F and H, which plot very close together, are from the dredge SD-7 oceanites (Figure 2) and the dredge DS-3 aphyric olivine tholeiites (Figure 9), respectively. Olivine (+ plagioclase) is responsible for shifting residual compositions from analogs of these parental types, to compositions such as glass Group R (DSDP Site 429), at an intermediate point on the sharply curved trend. In Site 429 basalts, olivine is still a minor mineral, but modes are dominated by plagioclase and clinopyroxene (Table 15, East Pacific Rise Site Report, this volume). Decline of olivine fractionation and ascendancy of clinopyroxene fractionation then shift residual compositions toward the quartz apex, although on this projection, some olivine fractionation must still occur to move compositions into the quartz-normative field. Thus, basalts corresponding to glass Groups A, C, K, Q, and S of Natland and Melson (this volume) still have minor modal olivine (Batiza et al., 1977; East Pacific Rise Site Report, this volume). Finally, the quartz-normative glasses all have microphenocrysts of clinopyroxene and plagioclase, chiefly as clusters in glassy and spherulitic samples, and correspond to the ferrobasalts depicted on Figure 7.

These comparisons suggest that microphenocrysts (plagioclase + olivine and/or clinopyroxene), particularly those in multiphase clusters, are a good petrographic guide to the degree of evolution of abyssal tholeiites. Although the rate of cooling of the basalts when these crystals formed might have been fairly high, nevertheless the profound effects of undercooling experienced during pillow or sheet flow formation had not yet occurred. Nor are these crystals likely to be xenocrysts added to the magma during mixing. The correspondence of microphenocrysts to the minerals that can be infered to control fractionation based on the normative plot (Figure 15) is very good. Even the olivine-spinel phyric oceanites and tholeiites have at least incipient plagioclase microlite formation to suggest that cotectic crystallization of olivine and plagioclase had begun. Consequently, there are no glass compositions that can be linked by fractionation of olivine (+ spinel) alone; some plagioclase fractionation is also necessary (see MgO variation diagrams, Natland and Melson's fig. 2, this volume).

Ferrobasalts can also be distinguished from olivine tholeiites by several other criteria, which will corroborate indications from microphenocrysts. These are: (1) nearly opaque coalesced spherulites; (2) tiny abundant titanomagnetites in the coalesced spherulites; (3) coarse titanomagnetites in high concentrations in interstitial zones of subophitic rocks; and (4) abundant, large, globular sulfides associated with titanomagnetite in coarser grained samples.

To distinguish olivine tholeiites from the more alkalic olivine basalts is made more difficult by my having examined only one example of the latter. The two extremes represent nearly the entire variation caused by differences in depth or degree of melting, and source heterogeneities, in the region ("band-width" variations of Natland and Melson, this volume; trend 2 of Figure 15). Only some basalts of dredge SD-8 (not described) are more alkalic (Batiza et al., 1977). The major difference between olivine tholeiites and the more alkalic basalts is the lack in the latter of even the tiniest plagioclase

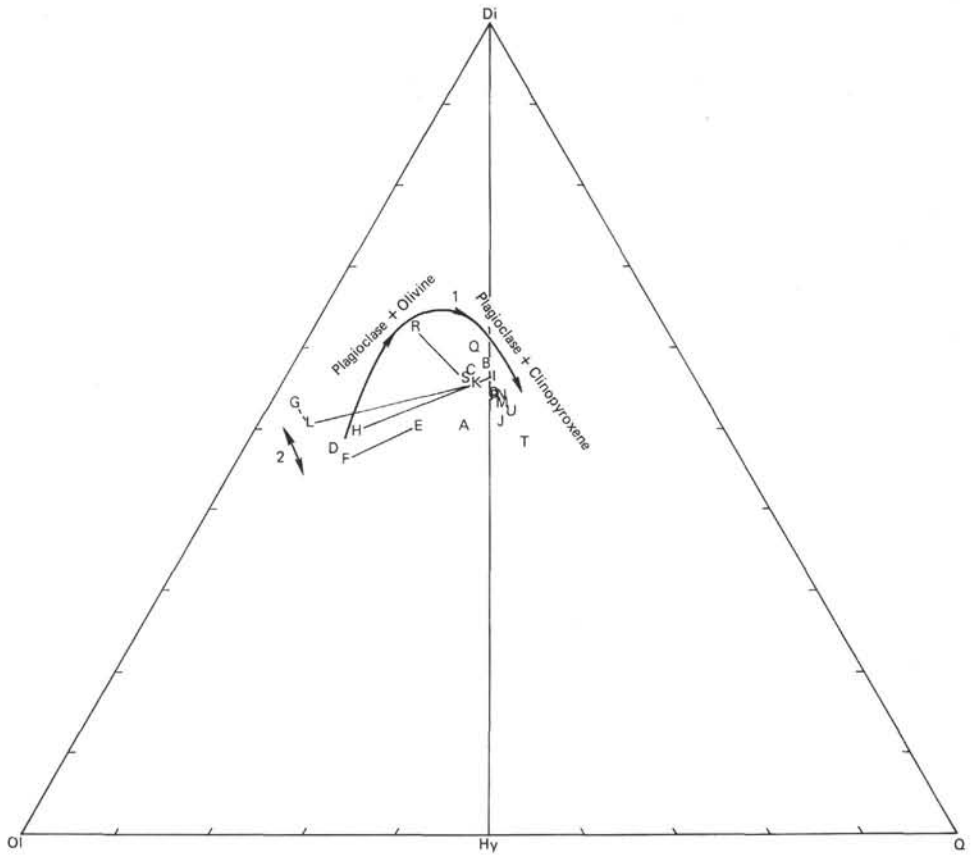

Figure 15. *Ternary plot of normative diopside (Di), olivine (Ol), hypersthene (Hy), and quartz (Q) for glass compositions of Table 3 of Natland and Melson (this volume). Groups A–S: East Pacific Rise near 9°N and the Siqueiros fracture zone; Group T: Galapagos Rift, Site 424; Group U: East Pacific Rise 3°25′S. Trend 1 is the generalized path of normative compositions as a result of crystal fractionation, first of plagioclase and olivine, then of plagioclase and clinopyroxene. Trend 2 (double-headed arrow) shows approximate range in normative compositions of probable parental olivine tholeiites that result from variations in the depth or degree of melting, and source heterogeneities. Groups G and L (linked by dashed line) are more alkalic seamount basalts. Groups linked by solid lines are from the same dredge haul or drill site.*

microlites in glass or the zone of coalesced spherulite globules. The occurrence of small, euhedral olivine microphenocrysts, but not granular megacrysts and glomerocrysts, is also distinctive, but the significance of the size and morphology is uncertain. More important is the abundance of these olivine phenocrysts throughout the samples, and the abundance of swallowtail olivine in microlitic zones. This feature is reminiscent of one of the classical distinctions between subaerial tholeiites and alkalic olivine basalts: the latter have *groundmass* olivine. What seems to be occurring in a rather subtle way is that the overall abundance of plagioclase is lower, and that of olivine is higher, at all stages of crystallization, than in olivine tholeiites. This is because the basalt has less CaO, less SiO_2, and more Na_2O than abyssal tholeiites at comparable MgO (Natland and Melson, this volume). In terms of phase petrology, this would tend to broaden the temperature interval between the onset of olivine crystallization, and the onset of plagioclase crystallization, a feature which would probably persist or be extended at heightened undercoolings (see fig. 2 of Walker et al., 1976). The higher CaO may also influence the formation of incipient clinopyroxene spherulites in these basalts where they do not generally occur among olivine tholeiites.

A summary of the principal petrographic features of the basalts described in this paper is given on Table 2.

Magma Mixing and Comparisons with Mid-Atlantic Ridge Basalts

The suite of samples described here offers little petrographic indication that magma mixing has occurred. This is surprising because of the geophysical evidence for a steady-state magma chamber of considerable dimensions (underlying the entire axial block) on this portion of the East Pacific Rise (cf. Rosendahl, 1976). In such a reservoir, replenished only from deeper sources, magma mixing certainly must occur (O'Hara, 1977;

TABLE 2
Summary of Petrographic Features of Basalts Described in the Text

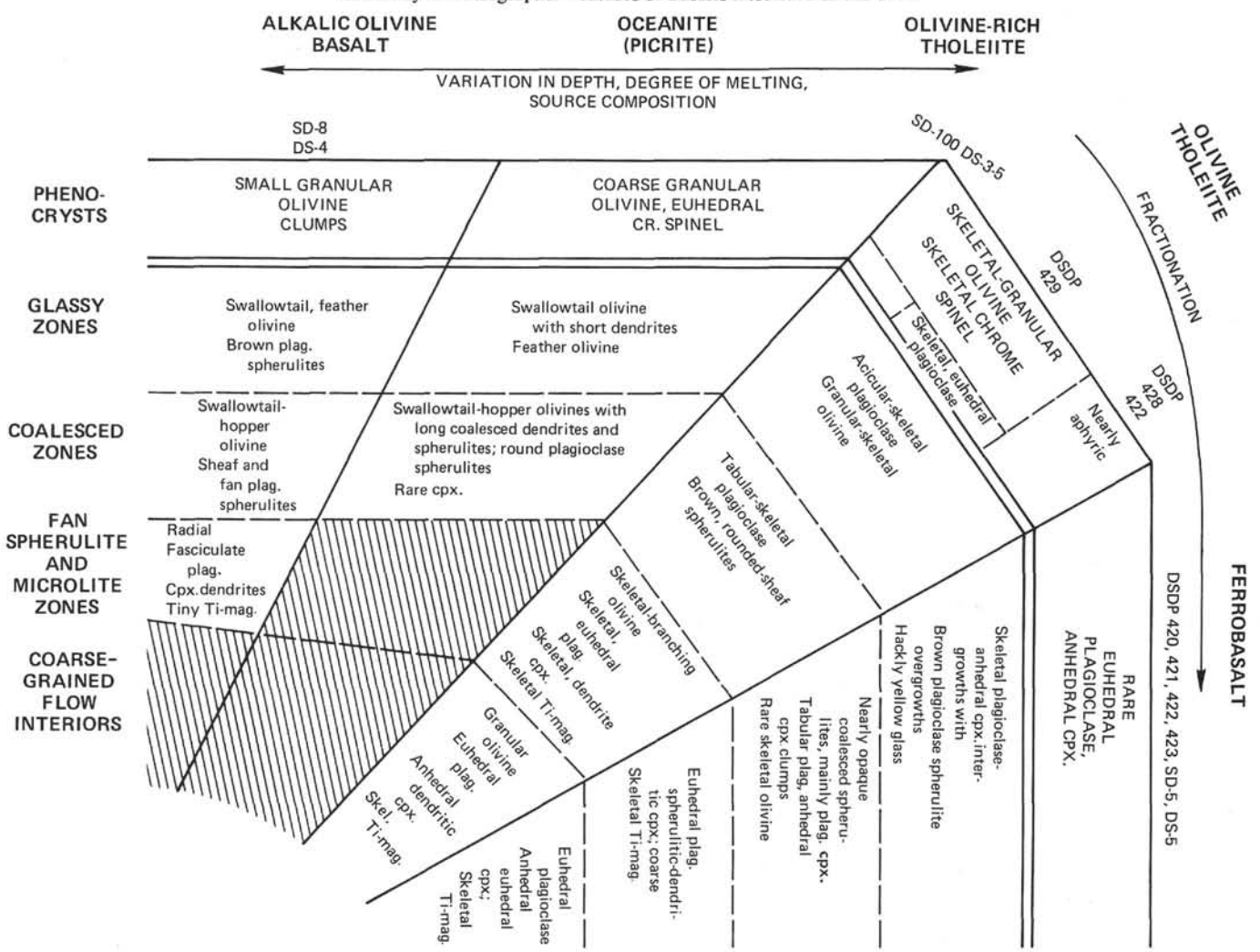

Bryan et al., 1979). The lack of evidence for mixing is largely because so few of the samples contain large megacrysts with glass inclusions such as have provided powerful evidence for mixing among Mid-Atlantic Ridge magmas (e.g., Dungan and Rhodes, 1978). Only the plagioclase–olivine phyric basalts from the Siqueiros fracture zone show analogous features.

This lack of petrographic evidence for mixing may depend in part on a critical lack of certain compositions available for study. Basalts from the Siqueiros fracture zone are dominated by primitive olivine tholeiites [Mg/(Mg + Fe) = 0.63–0.71 in glasses]. Those from the East Pacific Rise crest and flanks are predominantly ferrobasalts [Mg/(Mg + Fe) <0.55]. Even olivine tholeiites from the Rise are rather highly evolved, with low normative olivine in their glasses (Figure 15). There are few intermediate compositions to bridge the gap between these (glass Group R from Site 429 is one exception). Given the available end members, such intermediate compositions would seem to be the logical products of magma mixing; but we do not have them to study.

Two possible petrographic effects involving mixing of primitive and evolved abyssal tholeiites have been suggested by Walker et al. (1979). The first stems from the curvature of the liquidus boundary in the system $CaO–MgO–Al_2O_3–SiO_2$, defined by projection of normative compositions of experimentally determined compositions into various planes of the CMAS system. The curvature of the natural glass fractionation trend of Figure 15, and of several MgO variation diagrams (Natland and Melson, this volume) is analogous to this. If mixing occurs between two end members on this curve, the hybrid will not lie on the curve but within the primary phase volume of clinopyroxene. Mixing will have supercooled the hybrid, forcing crystallization of clinopyroxene. This predicts coexistence of clinopyroxene and olivine phenocrysts in basalts which would otherwise only have had olivine as a mafic phenocryst. No such clinopyroxene-bearing basalts occur among the East Pacific Rise samples, although several of the phyric groups from DSDP Site 395 on the Mid-Atlantic Ridge have clinopyroxene phenocrysts. On other evidence, those basalts are considered to be hybrids (Dungan et al., 1978; Natland, 1978).

Walker et al. (1979) also considered that, depending on what end members are involved in mixing, departure

from cotectic boundaries could result in superheated or supercooled magmas, with important, but not necessarily guaranteed, contrasts in texture. A magma that is supercooled by this mechanism will have many centers of crystal nucleation, and should crystallize to a mesh or subophitic texture. A hybrid magma that is superheated by this mechanism should have fewer centers of nucleation (as already discussed in another context), and form fewer crystals that are extremely elongate at comparable undercoolings. This is called fasciculate texture. Among Mid-Atlantic Ridge Site 395 aphyric basalts, both these textures occur. Types A_3 and A_4 have mesh and type A_2 fasciculate textures (see illustrations in Natland, 1978). Both types A_2 and A_3 appear to be hybrid compositions, based on geochemical evidence (Rhodes and Dungan, 1979; Natland, this volume).

The key to developing fasciculate texture among abyssal tholeiites, using the phase petrologic arguments of Walker et al. (1979), is to mix lavas having, besides plagioclase, either olivine alone or olivine and high-Ca clinopyroxene on the liquidus, with highly evolved ferrobasalts having low-Ca clinopyroxene (pigeonite) on the liquidus. Owing to an inflection in the liquidus boundary, such mixing causes the hybrids to be superheated; hence fasciculate textures are developed. The evolved basalts evidently have 14–18 per cent FeO* and 2.5–4.5 per cent TiO_2. Now all the aphyric East Pacific Rise or flank basalts examined for this study have mesh or subophitic textures, and none is as evolved as these. This suggests that highly evolved compositions are very rarely produced along this portion of the Rise, and that none was involved in mixing to produce the ferrobasalts we have recovered. Therefore, the sampled ferrobasalts in all likelihood are themselves close to the maximum residual compositions produced in any abundance in this region, and resulted from crystal fractionation.

Walker et al. (1979) have stressed that mixing in axial magma reservoirs should produce on average an intermediate hybrid composition far more abundant than typical residual iron-enriched magma types. They found data to support this in compilations of worldwide abyssal tholeiites. The conclusion just reached, however, seems to contradict this, since ferrobasalts are so abundant in the Leg 54 study area but are at the upper end of the spectrum in terms of degree of fractionation.

Elsewhere, I have presented geochemical data which show that mixing between East Pacific Rise primitive olivine tholeiites and ferrobasalts does not occur (Natland, this volume). The presence of an axial magma chamber seems to buffer the composition of primitive magmas supplied at its base to only somewhat more evolved olivine basalt magmas. Ferrobasalts themselves appear to form in isolated small magma bodies (dikes, lava lakes, trapped magma pockets) above or away from the main body of the magma chamber. Mixing within the magma chamber is thus among olivine tholeiite compositions only. Walker et al.'s (1979) arguments would favor some supercooling among hybrids of this mixing. This is not contradicted by textural evidence, since all axial basalts have mesh or subophitic textures in coarser-grained samples.

Ferrobasalts rarely erupt on the Mid-Atlantic Ridge, but seem much more commonly to be involved in mixing than on the East Pacific Rise. The fasciculate Type A_2 aphyric basalts and the phyric basalts with clinopyroxene phenocrysts from Site 395 are two examples of this. Indeed, glass compositions in the latter (Melson, 1978) are quartz-normative and distinctly more iron-enriched than either their whole-rock bulk compositions or other aphyric basalts at the site would suggest (see Natland, Axial Magma Chambers chapter, this volume, fig. 8). They contain strongly zoned megacrysts of olivine and plagioclase with core compositions that must have equilibrated in a more primitive melt, and which also contain more primitive glass inclusions (Dungan et al., 1978). The clinopyroxene phenocrysts do not clump with these in glomerocrysts. Therefore, they formed during or after mixing between a megacryst-bearing primitive magma, and an evolved magma represented by the host glass compositions. Groundmass textures and crystal morphologies of these hybrids in many respects resemble those of East Pacific Rise ferrobasalts (Figures 12 and 13), especially in having abundant plagioclase and clinopyroxene but no olivine dendrites in glassy and spherulitic samples (Natland, 1978, fig. 13).

The rarity of extreme differentiates among the worldwide abyssal tholeiite population does not, in my view, arise because of the general development of recurrently replenished steady-state axial magma chambers. On the contrary, most of the analyzed abyssal tholeiite population is from rifted, slow-spreading ridges. For one such ridge, the Mid-Atlantic, geophysical evidence (Rosendahl, 1976; Nisbet and Fowler, 1978; Sleep and Rosendahl, 1979), structure (Allmendinger and Riis, 1979) and petrologic inferences (Rhodes et al., 1978; Bougault et al., 1978; Natland, 1978) point to the existence of small, isolated, infrequently replenished magma chambers. These were so close together that they supplied distinct batches of lava with contrasting chemistry to the same DSDP sites either simultaneously or alternately throughout the construction of Layer 2 (Natland, 1978 and this volume). The magma types cannot be related by crystal fractionation or accumulation. The inference that mixing is involved in producing median compositions is correct. But this is because mixing between primitive and evolved end members at both deep and shallow levels in the crust is favored on the Mid-Atlantic Ridge. On the East Pacific Rise, however, the buffering axial magma reservoir ensures that such mixing of extreme end members cannot occur. This view is developed more fully in Natland (Axial Magma Chambers, chapter, this volume).

In summary, geochemical data imply that certain types of magma mixing do not occur in the axial magma chamber of the East Pacific Rise near 9°N. This is not contradicted in any sample by mineralogical or textural evidence. Olivine tholeiites can mix with olivine tholeiites, and possibly ferrobasalts with other ferrobasalts (in shallow conduits prior to eruption). But primitive olivine tholeiites and ferrobasalts do not mix. Basalts that are enriched with iron to an extreme extent rarely, if at

all, erupt, since none has been sampled, and none can be inferred to have mixed with any more primitive magma on the basis of textural evidence.

ACKNOWLEDGMENTS

I would like to thank my Leg 54 shipboard colleagues for many discussion on the merits and demerits of using crystal morphologies as an aid to petrographic identification of rock types. They may remember a briefer version of this as "A Poor Man's Guide to Geochemical Discriminants." Special thanks are due to the skillful crew of marine technicians aboard the *Glomar Challenger* during Leg 54 who made so many excellent thin sections, to Jeff Johnson, for lending me the collection of Deepsonde samples and thin sections, and to Ed Schrader and Bruce Rosendahl for sending me samples of the "oceanites." Dave Ripley made two especially fine polished sections of dredged samples for me. I also thank Jim Kirkpatrick for numerous discussions of the mechanisms of crystal growth, and for sending me a copy of Lung-Chuan Kuo's thesis.

REFERENCES

Allmendinger, R. W., and Riis, F., 1979. The Galapagos Rift at 86°W, 1, Regional morphological and structural analysis. *J. Geophys. Res.,* v. 84, p. 5379–5389.

Batiza, R., Rosendahl, B. R., and Fisher, R. L., 1977. Evolution of oceanic crust, 3, petrology and chemistry of basalts from the East Pacific Rise and the Siqueiros transform fault. *Ibid.,* v. 82, p. 265–276.

Battacharji, S., and Smith, C. H., 1964. Flowage differentiation. *Science,* v. 145, p. 150–153.

Bougault, H., Cambon, P., Joron, L., and Treuil, M., 1978. Trace elements: fractional crystallization and partial melting processes, heterogeneity of upper mantle material. *In* Melson, W. G., Rabinowitz, P. D., et al., *Initial Reports of the Deep Sea Drilling Project,* v. 45: Washington (U.S. Government Printing Office), p. 247–252.

Bryan, W. B., 1972. Morphology of quench crystals in submarine basalts. *J. Geophys. Res.,* v. 77, p. 5218–5819.

Bryan, W. B., Thompson, G., and Michael P. J., 1979. Compositional variation in a steady-state zoned magma chamber: Mid-Atlantic Ridge at 36°50′N. *Tectonophysics,* v. 55, p. 63–85.

Coleman, R. G., 1977. *Ophiolites:* New York (Springer-Verlag).

Corliss, J., Gordon, L. I., and Edmond, J. M., 1979. Some implications of heat/mass ratios in Galapagos Rift hydrothermal fluids for models of sea water — rock interaction and the formation of oceanic crust. *In* Talwani, M., Harrison, C., and Hayes, D. E. (Eds.), *Deep Drilling Results in the Atlantic Ocean: Ocean Crust,* Maurice Ewing Series 2: Washington (American Geophysical Union), p. 383–390.

Crane, K., 1976. The intersection of the Siqueiros transform fault and the East Pacific Rise. *Mar. Geol.,* v. 21, p. 25–46.

Delaney, J. R., Muenow, D. W., and Graham, D. G., 1978. Abundance and distribution of water, carbon, and sulfur in the glassy rims of submarine pillow basalts. *Geochim. Cosmochim. Acta.,* v. 42, p. 581–594.

Donaldson, C. H., 1976. An experimental investigation of olivine morphology. *Contrib. Mineral. Petrol.,* v. 57, p. 187–213.

_____, 1979. An experimental investigation of the delay in nucleation of olivine in mafic magmas. *Ibid.,* v. 69, p. 21–32.

Drever, H. I., and Johnston, R., 1958. The petrology of picritic rocks in minor intrusions — a Hebridean group. *Trans. Roy. Soc. Edinburgh,* v. 63, p. 459–499.

Dungan, M. A., Long, P. E., and Rhodes, J. M., 1978. The petrology, mineral chemistry and one-atmosphere phase relations of basalts from Site 395. *In* Melson, W. G., Rabinowitz, P. D., et al., *Initial Reports of the Deep Sea Drilling Project,* v. 45: Washington (U.S. Government Printing Office), p. 461–478.

Dungan, M. A., and Rhodes, J. M., 1978. Residual glasses and melt inclusions in basalts from DSDP Legs 45 and 46: evidence for magma mixing. *Contrib. Mineral. Petrol.,* v. 67, p. 417–431.

Fujii, T., Kushiro, I., and Hamuro, K., 1978. Melting relations and viscosity of an abyssal olivine tholeiite. *In* Melson, W. G., Rabinowitz, P. D., et al., *Initial Reports of the Deep Sea Drilling Project,* v. 45: Washington (U.S. Government Printing Office), p. 513–516.

Gibb, F. G. F., 1974. Supercooling and the crystallization of plagioclase from a basaltic magma. *Mineral. Mag.,* v. 39, p. 641–653.

Hopson, C. A., Pallister, J. S., Coleman, R. G., and Bailey, E. B., 1977. Geological section of the Semail ophiolite near Ibra, southeastern Oman Mountains, Sultanate of Oman. *Geol. Soc. Am. Abstr.,* v. 9, p. 1024–1025.

Johnson, J., 1979. Transitional basalts and tholeiites from the East Pacific Rise, 9°N. *J. Geophys. Res.,* v. 84, p. 1635–1025.

Kirkpatrick, R. J., 1978. Processes of crystallization in pillow basalts, Hole 396B, DSDP Leg 46. *In* Dmitriev, L., Heirtzler, J., et al., *Initial Reports of the Deep Sea Drilling Project,* v. 46: Washington (U.S. Government Printing Office), p. 271–282.

Kirkpatrick, R. J., and Melchior, J., 1979. Crystal growth in programmed cooling experiments — diopside. *Geol. Soc. Am. Abstr.,* v. 11, p. 458.

Komar, P. D., 1972. Mechanical interactions of phenocrysts and flow differentiation of igneous dikes and sills. *Ibid.,* v. 83, p. 973–988.

Kuo, Lung-Chuan, 1980. Morphology and zoning patterns of plagioclase in phyric basalts from DSDP Legs 45 and 46, Mid-Atlantic Ridge [Unpublished M.Sc. Thesis]. University of Illinois.

Lofgren, G., 1971. Spherulitic textures in glassy and crystalline rocks. *J. Geophys. Res.,* v. 76, p. 5635–5648.

_____, 1974. An experimental study of plagioclase crystal morphology: isothermal crystallization. *Am. J. Sci.,* v. 274, p. 243–273.

Macdonald, G. A., 1949. Hawaiian petrographic province. *Geol. Soc. Am. Bull.,* v. 60, p. 1541–1596.

_____, 1968. Composition and origin of Hawaiian lavas. *Geol. Soc. Am. Mem.,* v. 116, p. 477–522.

Melson, W. G., 1978. Chemical stratigraphy of Leg 45 basalts: electron probe analyses of glasses. *In* Melson, W. G., Rabinowitz, P. D., et al., *Initial Reports of the Deep Sea Drilling Project,* v. 45: Washington (U.S. Government Printing Office), p. 507–511.

Moore, J. G., Batchelder, J. N., and Cunningham, C. G., 1977. CO_2-filled vesicles in mid-ocean basalt. *J. Volcanol. Geotherm. Res.,* v. 2, p. 309–327.

Muenow, D. W., Graham, D. G., Liu, N. W. K., and Delaney J. R., 1979. The abundance of volatiles in Hawaiian tholeiitic submarine basalts. *Earth Planet. Sci. Lett.,* v. 42, p. 71–76.

Natland, J. H., 1978. Crystal morphologies in basalts from DSDP Site 395, 23°N, 46°W, Mid-Atlantic Ridge. *In* Melson, W. G., Rabinowitz, P. D., et al., *Initial Reports of the Deep Sea Drilling Project,* v. 45: Washington, (U.S. Government Printing Office), p. 423–445.

Nisbet, E. G., and Fowler, C. M. R., 1978. The Mid-Atlantic Ridge at 37° and 45°N: some geophysical and petrological

constraints. *Geophys. J. Roy. Astron. Soc.*, v. 54, p. 631–660.

O'Hara, M. J., 1977. The geochemistry of lavas erupted from a magma chamber undergoing fractional crystallization with periodic addition and intermingling of more primitive magma. *Nature*, v. 266, p. 503–507.

Rhodes, J. M., Blanchard, D. P., Dungan, M. A., Rodgers, K. V., and Brannon, J. C., 1978. Chemistry of Leg 45 basalts. *In* Melson, W. G., Rabinowitz, P. D., et al., *Initial Reports of the Deep Sea Drillinig Project*, v. 45: Washington (U.S. Government Printing Office), p. 447–460.

Rhodes, J. M., and Dungan, M. A., 1979. The evolution of ocean-floor basaltic magmas. *In* Talwani, M., Harrison, C. G., and Hayes, D. E. (Eds.), *Deep Sea Drilling Results in the Atlantic Ocean: Ocean Crust*, Maurice Ewing Series 2: Washington (American Geophysical Union), p. 262–272.

Rosendahl, B. R., 1976. Evolution of oceanic crust 2: constraints, implications, and inferences. *J. Geophys. Res.*, v. 81, p. 5305–5314.

Schweitzer, E. L., Papike, J. J., and Bence, A. E., 1979. Statistical analysis of clinopyroxenes from deep-sea basalts. *Am. Min.*, v. 64, p. 501–513.

Shaw, H. R., 1972. Viscosities of magmatic silicate liquids: an empirical method of prediction. *Am J. Sci.*, v. 272, p. 870–893.

Simkin, T., 1967. Flow differentiation in the pictiric sills of north Skye. *In* Wyllie, P. J. (Ed.), *Ultramafic and Related Rocks:* New York (John Wiley & Sons), p. 64–69.

Sleep, N. H., and Rosendahl, B. R., 1979. Topography and tectonics of mid-oceanic ridge axes. *J. Geophys. Res.*, v. 84, p. 6831–6839.

Sparks, R. S. J., Meyer, P., and Sigurdsson, H., 1980. Density variation amongst mid-ocean ridge basalts: implications for magma mixing and the scarcity of primitive lavas. *Earth Planet. Sci. Lett.*, v. 46, p. 419–430.

Walker, D., Kirkpatrick, R. J., Longhi, J., and Hays, J. F., 1976. Crystallization history of lunar picritic basalt sample 12002: phase equilibria and cooling-rate studies. *Geol. Soc. Am. Bull.*, v. 87, p. 646–656.

Walker, D., Shibata, T., and DeLong, S. E., 1979. Abyssal tholeiites from the Oceanographer fracture zone II. Phase equilibria and mixing. *Contrib. Mineral. Petrol.*, v. 70, p. 111–125.

APPENDIX

Sector-Zoned Olivine: A Correction

Colin H. Donaldson and James H. Natland

Natland (1978) reported and figured a sector-zoned crystal in a feldspar phyric basalt which from circumstantial evidence (parallel extinction; lack of clinopyroxene megacrysts in the basalt unit sampled) he identified as olivine. One of us (C.H.D.) was skeptical of, and intrigued by, this identification, because to his knowledge sector-zoned crystals of olivine had never before been reported, unlike the other basaltic minerals augite and plagioclase. Accordingly, Donaldson was sent the thin section (Sample 395A-15-1, 55–58 cm) containing the crystal, and he obtained the energy-dispersive electron probe analyses of the crystal which are shown in Table 1. It can be seen that the crystal in augite, typical of augites in tholeiites (i.e., with relatively low Al and Ti contents [cf., Schweitzer et al., 1979], although with 1–1.5 per cent more CaO than the tholeiitic augites listed by those reviewers). Of note are the only slight differences in Al, Ti, Fe and Mg between core and rim of the crystal and between the different sectors.

Despite this negative finding, we hope that those examining rapidly cooled basalts, such as oceanic basalts, will be alerted to look for sector-zoned olivines. Cursory examination might result in misidentification of such crystals as pyroxene. However, we hold out little hope that sector-zoned olivine will ever be found (a) because of the mineral's "straightjacket" composition (i.e., Si is virtually unchallenged for the tetrahedral sites and Mg and Fe have little competition for the octahedral sites); and (b) because Mg^{2+} and Fe^{2+} ions diffuse in the melt at very similar rates, owing to their similar ionic radii, such that they are not preferentially fractionated into different sectors growing at different rates.

TABLE 1
Electron-Probe Analyses of Sector-Zoned Crystal in Sample 395A-15-1, 55–58 cm

	Core of Sector 100	Rim of Sector 100	Core of Sector 001
SiO_2	52.73	51.24	52.61
TiO_2	0.67	0.91	0.47
Al_2O_3	2.33	3.31	1.95
Cr_2O_3	0.66	0.54	0.60
FeO*	5.81	6.46	5.40
MnO	0.13	0.25	0.13
MgO	17.31	16.50	17.83
CaO	20.26	20.31	20.14
Na_2O	<0.10	<0.10	<0.10
Total	99.90	99.52	99.13
	Structural Formulae		
Si	1.929	1.895	1.937
Al^{IV}	0.071	0.105	0.063
Al^{VI}	0.030	0.040	0.021
Ti	0.019	0.026	0.013
Cr	0.019	0.016	0.018
Fe	0.178	0.200	0.166
Mn	0.005	0.008	0.004
Mg	0.944	0.910	0.977
Ca	0.794	0.805	0.793
Total	3.989	4.005	3.992

Note: Analyses made on the Edinburgh University Mark V electron microprobe.
*All Fe as FeO.